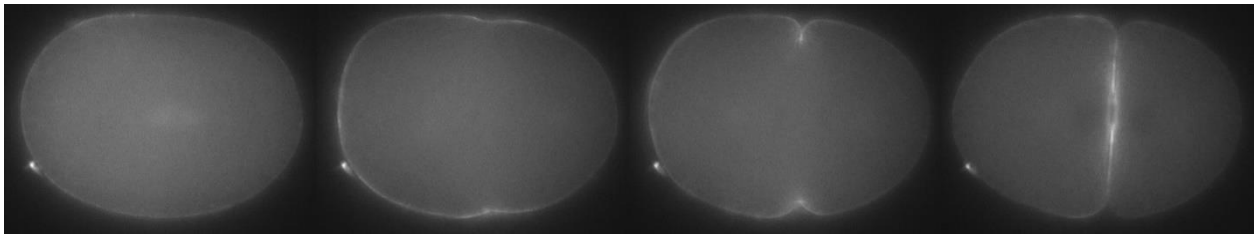

Phospho-regulation of myosin regulatory light chain in *Caenorhabditis elegans* embryos during cytokinesis

Joana Filipa Silva Saramago
Mestrado em Biologia Molecular e Celular
Departamento de Biologia
2014
Orientador
Ana Xavier Carvalho, PI, Instituto de Biologia Molecular e Celular
Coorientador
Ana Marta Silva, PhD, Instituto de Biologia Molecular e Celular

Todas as correções determinadas pelo júri, e só essas, foram efetuadas.
O Presidente do Júri,

Porto, _____/_____/_____

Acknowledgements

Gostaria de agradecer a todos os membros do grupo *Cytoskeletal Dynamics,* em especial à Ana Xavier Carvalho, pelo voto de confiança, pelo companheirismo, pela solidariedade e pela entreajuda. Pela amizade nos bons e maus momentos. Cresci imenso desde que cheguei há um ano ao nosso laboratório e, sem saber do futuro, espero poder continuar a crescer do vosso lado. Para mim, a ciência tornou-se mais fascinante.

Quero também agradecer aos membros do *Cell Division Mechanisms* por toda a ajuda e companheirismo.

Um especial agradecimento aos meus familiares, especialmente aos meus pais. Tudo o que sou hoje devo-vos a vós. Por toda a dedicação, por toda a preocupação, por serem capazes de me aturarem quando ando stressada. Na realidade não poderia pedir mais de vós, são um grande modelo de humildade, amor e capacidade de sacrifício para um bem maior. No futuro espero ser como vocês e ser capaz de retribuir tudo que fizeram por mim. Amo-vos!

Ao meu namorado, Jorge Oliveira, por estar presente sempre que preciso. Pelo teu amor e pela tua amizade. Obrigado pelas noites ao meu lado enquanto eu escrevia esta dissertação. Sei que nos completamos. Ao nosso futuro que agora começa!

À minha melhor amiga, Ana Júlia, por ser aquela que independentemente do que seja, ser capaz de me animar e de me mostrar o lado positivo da vida. Desde que te conheci que me demonstras as prioridades na vida e como saber reagir ao que realmente é importante. És uma força da natureza. Perdoa-me por nesta fase não ter estado tão presente como desejava.

A mim, por ser capaz de aprender e de me tornar cada vez mais forte a cada obstáculo que ultrapasso.

À faculdade de ciências da universidade do porto e ao instituto de biologia molecular e celular, por acolherem e financiarem os meus sonhos.

Sumário

Citocinese é o processo que finaliza a divisão celular durante o qual o conteúdo de uma célula é dividido por duas células-filhas. A maioria das proteínas que se sabe estarem envolvidas em citocinese são altamente conservadas em seres vivos, e de algumas delas já se conhecem bastantes detalhes moleculares baseados em estudos *in vitro*. Contudo, na situação *in vivo*, a complexidade do sistema impera e a compreensão do processo continua muito pouco claro a nível molecular. Pensa-se que a proteína miosina não-muscular II seja o motor molecular da citocinese que gera a força necessária para a constrição do anel contráctil. Experiências *in vitro* demonstram que a atividade da miosina não-muscular II é regulada pela fosforilação da sua cadeia regulatória leve nos resíduos treonina17 e serina18. A fosforilação da cadeia regulatória leve torna a miosina não-muscular II competente para interagir com outras moléculas de miosina não-muscular II e formar filamentos bipolares que permitem a contractilidade da rede de filamentos de actina e miosina. Ainda assim, a contribuição da fosforilação da cadeia regulatória leve da miosina na citocinese contínua controversa. Esta parece ser crucial em células S2 de *D. melanogaster* mas desnecessária em S. *pombe* e *D. discoideum*. No presente estudo, tentamos desvendar o papel da fosforilação dos aminoácidos treonina17 e serina18 da cadeia regulatória leve da miosina durante a citocinese em embriões de *C. elegans*. Para tal, criámos estirpes de *C. elegans* que expressam a proteína *wild-type* MLC-4::GFP, ou a proteína mutada MLC-4 A17A18::GFP (não fosforilável) ou MLC-4 D17E18:GFP (fosfomimética) Todos os transgenes foram desenhados de forma a serem resistentes a ARN de interferência, permitindo a avaliação do processo de citocinese em embriões que expressam a MLC-4 *wild-type* ou mutantes quer na presença da proteína endógena, quer na sua ausência. A análise da montagem e constrição do anel contráctil demonstraram que a proteína *wild-type* MLC-4::GFP é capaz de atuar de igual forma à proteína endógena durante a citocinese. Na presença da forma MLC-4 não-fosforilável, a citocinese não ocorre. Em contraste, na presença da forma MLC-4 fosfomimética, a citocinese ocorre de forma semelhante a quando a forma MLC-4 *wild-type* é expressa. Os nossos resultados sugerem que, durante todo o processo de citocinese, os filamentos bipolares da miosina não-muscular II mantêm-se ativos pois tornam-se competentes para a contractilidade através fosforilação nos resíduos Treonina17 e Serina18. O conhecimento mais extensivo deste assunto terá implicações importantes para a compreensão dos mecanismos do anel contráctil e abcisão, a fase final da citocinese.

Palavras-chave: Citocinese; Miosina não muscular II; Cadeia regulatória leve da miosina; Fosforilação; C. elegans; Embrião unicelular**.**

Abstract

Cytokinesis is known as the final step in cell division during which the contents of one mother cell are partitioned into the two daughter cells. Although most of the proteins involved in cytokinesis are known and well conserved among organisms, cytokinesis is still poorly understood at the molecular level. Non-muscle myosin II (NMYII) is thought to be the molecular motor that drives constriction of the contractile ring during cytokinesis. *In vitro* experiments show that non-muscle myosin II activity is regulated by phosphorylation of its regulatory light chain (MRLC) on the residues Threonine 17 Serine 18. NMII activation is required for it to become competent to interact with other NMII molecules and form bipolar filaments that allow for acto-myosin contractility. The contribution of MRLC phosphorylation to cytokinesis is however controversial. It seems to be crucial in *Drosophila* S2 cells but unnecessary in yeast and *Dictyostelium*. In this study, we intended to gain insight into the role of Threonine17 and Serine18 MRLC phosphorylation during cytokinesis using the Caenorhabditis *elegans* early embryo as experimental model. To do that, we generated *C. elegans* strains expressing wild-type, non-phosphorylatable (A17A18) or phosphomimetic (D17E18) MLC-4::GFP mutants, using the MosSCI technique. As transgenes were engineered to be RNA interference (RNAi) resistant, we were able to evaluate cytokinesis in 1-cell embryos expressing wild-type MLC-4::GFP or the mutated forms in the presence or absence of the endogenous protein. Analysis of contractile ring assembly and constriction have shown that wild-type MLC-4::GFP is able to perform as well as the endogenous MLC-4 during cytokinesis and rescues embryonic viability. In the presence of non-phosphorylatable MLC-4, cytokinesis does not happen. In contrast, in the presence of phosphomimetic MLC-4 cytokinesis is completed as when *wild-type* MLC-4 is expressed. Our results suggest that once NMII bipolar filaments become competent for contractility by MLC-4 phosphorylation on residues Threonine17 and Serine18, they remain in the active state throughout cytokinesis. Further understanding of this issue will have important implications for the understanding of the mechanics of the contractile ring and abscission, the last stage of cytokinesis.

Key words: Cytokinesis; Myosin regulatory light chain; non-muscle myosin II; Phosphorylation; *C. elegans*; One-cell embryo.

Table of Contents

Movies Index

Movie 1 - MLC-4 depletion in embryos expressing NMY-2::GFP leads to cytokinesis slow-down and failure. Time-lapse of one-cell *C. elegans* embryos expressing NMY-2::GFP undergoing cytokinesis in the presence of endogenous mlc-4 (left) or after depletion of endogenous mlc-4 by RNAi (middle and right). 25 hours post mlc-4 dsRNA injection, embryos failed cytokinesis (middle). 23 hours post mlc-4 dsRNA injection, embryos completed cytokinesis but with slower kinetics (right). Images were taken every 10 seconds. Time is shown in minutes and zero corresponds to the time point before anaphase onset.

Movie 2 - Wild-Type MLC-4::GFP probe is functional. Time-lapse of one-cell *C. elegans* embryos expressing wild-type MLC-4::GFP undergoing cytokinesis in the presence of endogenous mlc-4 (left) or 44 hours post endogenous mlc-4 dsRNA injection (right). Both show similar cytokinesis behavior. Time is shown in minutes and zero corresponds to one time point before anaphase onset.

Movie 3 - MLC-4(T17S18AA)::GFP expression leads to cytokinesis slow -down and failure. Time-lapse of one-cell *C. elegans* embryos expressing MLC-4(T17S18AA)::GFP undergoing cytokinesis in the presence of endogenous mlc-4 (left) or after depletion of endogenous mlc-4 by RNAi (middle and right). . 35 hours post mlc-4 dsRNA injection, embryos failed cytokinesis (middle). 33 hours post mlc-4 dsRNA injection, embryos completed cytokinesis but with slower kinetics (right). Images were taken every 10 seconds. Time is shown in minutes and zero corresponds to one time point before anaphase onset.

Movie 4 - Endogenous MLC-4 gradual depletion in embryos expressing MLC-4(T17S18DE)::GFP. Time-lapse of one-cell *C. elegans* embryos expressing MLC-4(T17S18DE)::GFP undergoing cytokinesis in the presence of endogenous mlc-4 (left) or 33 hours after endogenous mlc-4 depletion (middle and right). After depletion of endogenous mlc-4 by RNAi, two distinct phenotypes were observed: embryos that completed cytokinesis with normal kinetics (group 1, middle) and embryos that presented a prolonged cytokinesis (group 2, right). Images were taken every 10 seconds. Time is shown in minutes and zero corresponds to one time point before anaphase onset.

List of Abbreviations

AMPK - AMP-activated protein kinase

ATP - Adenosine triphosphate

ATPase - Adenosine triphosphatase

C. elegans - *Caenorhabditis Elegans*

CR – Contractile Ring

DNA – Deoxyribonucleic Acid

dsRNA – double-strand RNA

dsRNA-endog - dsRNA targeting endogenous protein

E. coli - *Escherichia coli*

ELC - Essential light chain

EM - Electron microscopy

GFP - Green fluorescent protein

LHS - Left homologous sequence

MLCK - Ca^{2+}- calmodulin-dependent MLC kinase

MosSCI - Mos Single Copy Insertion

MRCK - Myotonic dystrophy kinase-related CDC42-binding kinase

MRLC/MLC-4 - Regulatory light chain

NGM - Nematode growth medium

NMII - Non-muscle myosin II

NMY-2 – *C. elegans n*on-muscle myosin II heavy chain

PCR - Polymerase chain reaction

RHS - Right homologous sequence

RNA – Ribonucleic acid

RNAi - RNA interference

ROCK - Rho kinase

ZIPK - Leucine zipper interacting kinase

1. Introduction

1.1. Cytokinesis

Cell division comprises cell growth and a well-organized series of events that include genome replication, chromosomal segregation, and cytokinesis (Glotzer M, 2005). Cytokinesis is the biological process by which one mother cell is physically partitioned into two daughter cells. A successful cytokinesis ensures that each daughter cell retains one copy of the replicated genome, and its failure gives rise to polyploidy cells recognized to be a critical intermediate in the development of cancer (Sagona and Stenmark, 2010). Most of the protein machinery involved in cytokinesis is known and is extremely well conserved among organisms but cytokinesis is still poorly understood at the molecular level.

In animal cells, cytokinesis is dependent on a contractile ring that assembles beneath the plasma membrane and generates a cleavage furrow that divides the mother cell into two (Figure 1) (Glotzer M, 2005). Cues from the anaphase spindle define the cleavage site where the contractile ring is assembled at the cell equator. When the contractile ring is assembled, it starts constricting, bringing the plasma membrane behind it, which generates a barrier between the two daughter cells. By the end of constriction, the contractile ring reaches the mitotic spindle microtubules at the midzone. The contractile ring transitions into a midbody ring and the abscission machinery completely seals the final gap between the two daughter cells (Green et al., 2012).

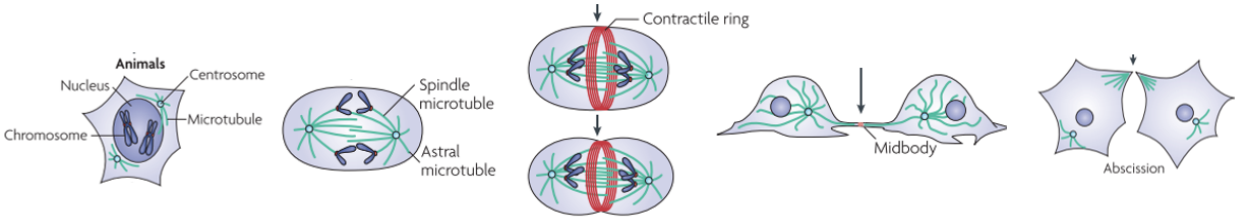

Figure 1 - Schematic of cytokinesis in animal cells. Cytokinesis leads to the physical division of one cell into two. Animal cells assemble a contractile ring of actin filaments and myosin II around the cell equator between the two masses of segregated chromosomes, which are separated by microtubules of the mitotic apparatus. The ingressing furrow compacts the spindle midzone into a dense structure called the midbody, and then complete daughter cell separation occurs in abscission. (Adapted from Pollard and Wu, 2010)

Electron microscopy observations in multiple systems show that the contractile ring is a thin layer (0.1-0.2 µm) of a filamentous network composed of actin filaments organized circumferentially and with mixed polarities (Schroeder T.,1968, 1970, 1972; Selman G. and Perry M., 1970; Arnold J., 1969; Tucker J.,1971; Maupin P. and Pollard T., 1986; Kamasaki et al., 2007). Filaments of non-muscle myosin II (NMII) and septins also compose the contractile ring (Figure 2). Other proteins that compose the contractile ring include actin regulators involved in elongating, severing, capping and cross-linking actin filaments as well as NMII binding partners.

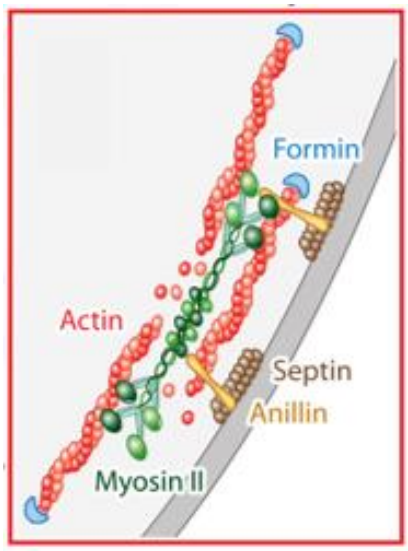

Figure 2 - **Contractile ring components.** In red, actin filaments nucleated by formins (blue), bipolar filaments of the motor non-muscle myosin II (green), septin filaments (brown), and the filament cross-linker anillin (yellow). (Adapted from Green et al., 2012)

1.2. Non-muscle myosin II and associated regulatory light chain in the contractile ring

In analogy to skeletal muscle, it has been proposed that contractile ring contractility is powered by a ‘‘sliding filament’’ mechanism in which bipolar NMII filaments pull actin filaments past one another (Schroeder, 1975). This view has been challenged recently, with reports that NMII could have a more passive role in the contractile ring, acting as a cross-linker to exert tension (Ma et al., 2012). One way or the other, NMII does play essential roles during cytokinesis as its inhibition by microinjection of anti-NMII antibodies or use of small molecule inhibitors, and genetic perturbations all inhibit furrow ingression leading to cytokinesis failure and consequent

multinucleation (Mabuchi & Okuno 1977, De Lozanne A. and Spudich J, 1987; Guo and Kemphues 1996, Karess et al. 1991, Shelton et al. 1999, Young et al. 1993).

NMII consists of a homodimer of heavy chains, each bound to an essential light chain (MELC) and a regulatory light chain (MRLC) (Figure 3). Bipolar filaments form by oligomerization of multiple homodimers and this process is regulated by phosphorylation of the MRLC and the heavy chain.

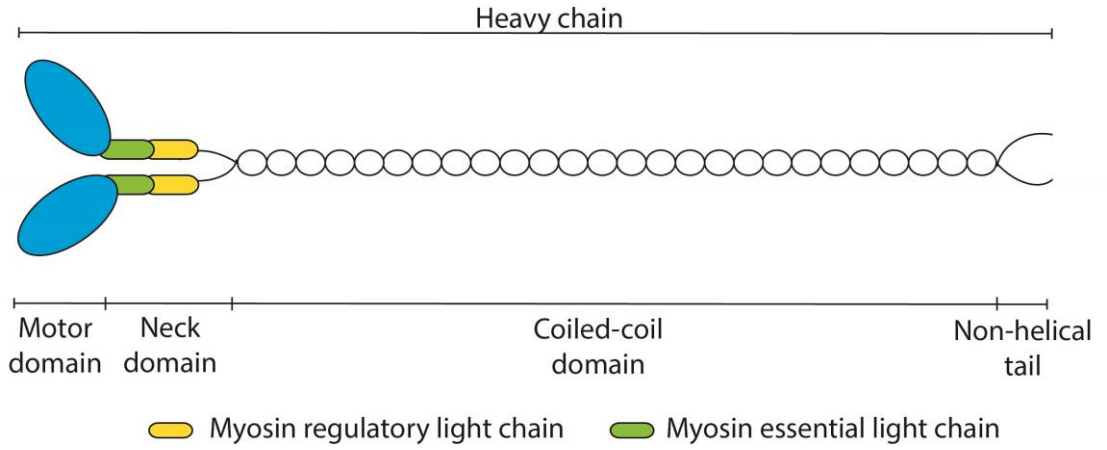

Figure 3 - Schematic of Non-Muscle Myosin II (NMII) structure. NMII is composed of a dimer of heavy chains. Each heavy chain binds one essential-light chain (MELC) for stabilization, and one regulatory light chain (MRLC) for regulation. The heavy chain comprises three regions: a motor domain that has ATPase activity and binds actin filaments, a neck domain where the light chains bind, a coiled-coil domain that enables dimerization and bipolar filament formation and a tail domain.

In animal cells, the regulation of NMII and smooth muscle myosin, but not cardiac or skeletal muscle myosin, is thought to depend on the reversible phosphorylation of the MRLC on the residues Threonine 17 and Serine 18, which have been evolutionary conserved (Figure 4).

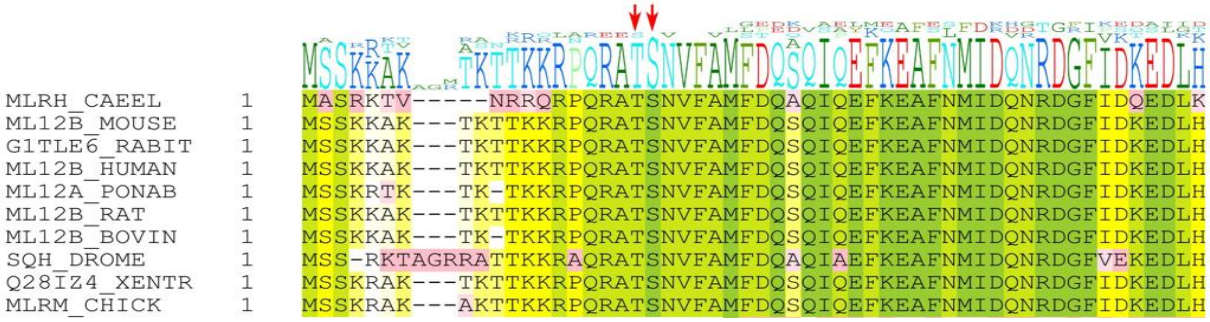

Figure 4 - Conservation of MRLC in several organisms. Serine 17 and threonine 18 (red arrows) are well conserved between different organisms (from top to bottom: *C. elegans, M. musculus, O. cuniculus H. sapiens, S. pombe, R. norvegicus, B. taurus, D. melanogaster, X. tropicalis, G. gallus*)

The non-phosphorylated NMII homodimer folds into a compact conformation. Upon phosphorylation of MRLCs in the residues Threonine 17 and Serine 18, the dimer unfolds and formation of NMII bipolar filaments is promoted. Formation of bipolar filaments is thought to be essential for contractility as they are competent to interact with actin filaments, and this interaction triggers the adenosine triphosphatase (ATPase) activity of NMII. The ATPase activity of NMII allows it to use the energy released by ATP hydrolysis to generate force and translocate the actin filaments (Figure 5) (Wendt et al., 2001; Woodhead et al., 2005; Jung et al., 2008; Craig and Woodhead, 2006; Burgess S et al., 2007).

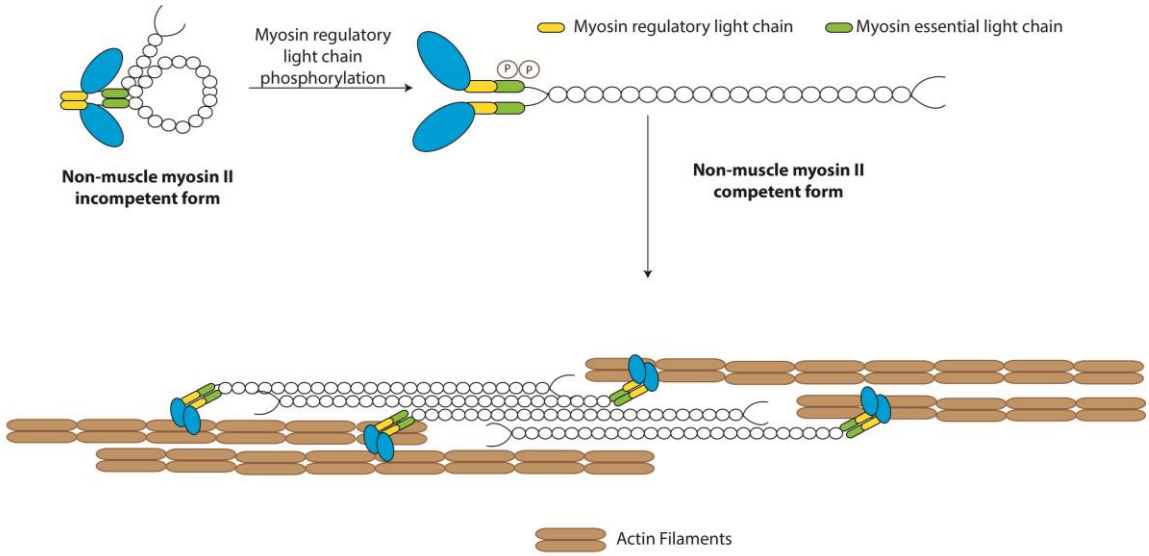

Figure 5 - **MRLC phosphorylation changes NMII conformation in order to promote bipolar filament formation.** MRLC phosphorylation in the residues Serine 17 and Threonine 18 leads to NMII dimer unfolding. The unfolded dimer is competent to establish interactions with other unfolded dimers through their coiled-coil regions. Bipolar filaments arise and can translocate actin filaments past one another. Change NMYII in figure to NMII.

Although these conformational changes of NMII by MRLC phosphorylation can be demonstrated in solution, there is no firm evidence that they occur *in vivo* (Vicente-Manzanares et al., 2009). In vitro studies have clearly shown that mono-phosphorylation of MRLC on Serine 19 can activate the ATPase activity of NMII and support actin motility while di-phosphorylation of MRLC on Threonine 17 and Serine 18, increases ATPase activity further more (Ikebe and

Hartshorne, 1985; Sellers et al., 1981; Trybus, 1989). Phosphorylation of MRLC can be performed by several kinases, including Rho kinase (ROCK), AMP-activated protein kinase (AMP kinase), Ca^{2+}-calmodulin-dependent MLC kinase (MLCK) (Sandquist et al., 2008; Kamm and Stull, 2001; Lee et al., 2010), leucine zipper interacting kinase (ZIPK), myotonic dystrophy kinase-related CDC42-binding kinase, and MRCK (Wilkinson et al., 2005; Leal et al., 2003). Only MLCK seems to be MRLC-specific, the other kinases are known to act in different cellular targets (Heissler and Manstein, 2013). MRLC de-phosphorylation by myosin phosphatases has the inverse effect on NMII leading to decreased contractile activity (Piekny and Mains, 2002). Myosin phosphatase activity is itself regulated by a variety of kinases, including Rho kinase (Conti and Adelstein, 2008; Ito el al., 2004) that enhances NMII activation both by inhibiting myosin phosphatase activity and by phosphorylating the MRLC (Kimura et al., 1996; Zhao and Manser, 2005; Matsumura, 2005).

The importance of MRLC phosphorylation on residues Threonine 17 and Serine 18, during cytokinesis is not clear. Phosphorylated Threonine 18 and Serine 19 has been detected in cytokinetic furrows of mammalian (DeBiasio et al., 1996; Matsumura et al., 1998; Asano et al., 2009) and *D. melanogaster* S2 cultured cells (Dean and Spudich, 2006). In S2 cells, expression of a non-phoshorylatable MRLC mutant where residues Threonine 20 and Serine 21 have been mutated to Alanines (correspond to *C. elegans* Threonine 17 and Serine 18) leads to cytokinesis failure and binucleated cells (Dean and Spudic, 2006). In HeLa cells, expression of non-phosphorylatable MRLC results in slower furrow ingression (Asano et al., 2009). Expression of di-phosphorylated MRLC in HeLa or S2 cells does not cause disruption in cytokinesis kinetics, indicating that cytokinesis occurs normally when NMII is active throughout (Dean and Spudic, 2006; Asano et al., 2009). *D. discoideum* cytokinesis is successful in the absence of MRLC (Zang et al., 1997; Uyeda et al., 1996) which suggest that fission yeast and *D. discoideum* use different mechanisms to regulate NMII bipolar formation (Ostrow et al., 1994; De la Roche et al.,2002;). In fact, it has been described that bipolar filament formation in *D. discoideum* is regulated by phosphorylation of NMII heavy chain (Bosgraaf and van Haastert, 2006). The relevance of heavy chain phosphorylation is however not clearly defined in mammalian cells.

1.3 Caenorhabditis elegans as biological model

Caenorhabditis elegans is an excellent experimental model system that has become increasingly used for research in the field of genomics, cell biology, neuroscience and ageing. *C. elegans* is a small, free-living soil nematode and subsists by feeding on microbes, primarily bacteria. Its maintenance in the laboratory is straightforward and non-expensive, as it can be

grown on agar plates with *E. coli* as food source. Other advantages that justify its widespread use are its short life cycle (Figure 6), compact genome, stereotypical development and transparency.

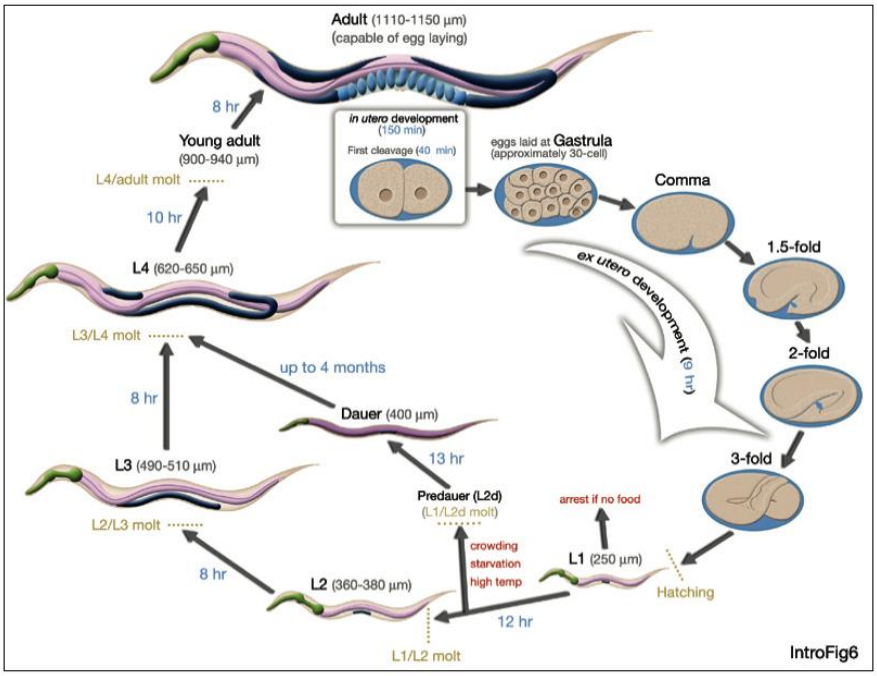

Figure 6 - Life cycle of *C. elegans* at 20 ºC. Time zero corresponds to fertilization. The time spent at each stage is shown in blue. First cell division happens 150 minutes after fertilization. One life cycle is completed in 3 days at 20 ºC.

C. elegans mostly exists as a self-fertilizing hermaphrodite (XX) but can also exist as male (XO). Males arise rarely in the natural population (0.1%) by spontaneous non-disjunction of chromosome X in the hermaphrodite germ line. Through mating, due to competition between male sperm and hermaphrodite sperm a higher frequency of males (up to 50%) can be easily achieved. Genetic crosses using *C. elegans* are straightforward and produce a large number of progeny per adult. Self-fertilization of the hermaphrodite allows for homozygous individuals to generate genetically identical progeny and male mating facilitates the isolation and maintenance of mutant strains as well as moving mutations between strains.

Strains can be kept as frozen stocks for long periods of time. *C. elegans* can switch to a facultative stage called dauer larva that can survive 4 to 8 times the normal 3-week life span (Cassada and Russell, 1975). Despite its simple anatomy, the animal is complex and displays a large range of behaviors including locomotion, foraging, feeding, defecation, egg laying, dauer larva formation, sensory responses to touch, smell, taste and temperature as well as some complex behaviors like male mating, social behavior, learning and memory (Rankin, 2002; de Bono, 2003).

The *C. elegans* genome has been completely sequenced and a comprehensive database including genes, phenotypes, mutants, and available strains exists.

The *C. elegans* early embryo is an extremely powerful biological system to conduct quantitative live imaging assays due to the stereotypical embryonic cell divisions. This is of great importance for the study of cell division and more specifically cytokinesis. In contrast to cell cultures, cellular divisions occur within the context of a multicellular organism, which constitutes a strong advantage. Cultured cells divide while adhered to a substrate, which may impose artificial constraints on cytokinesis that do not reflect the situation encountered in the context of a tissue.

Moreover, fluorescent versions of the protein of interest can be easily expressed in the embryo for fluorescent live imaging.

1.4 RNA interference

RNA interference (RNAi), first discovered and characterized in *C. elegans* (Fire et al., 1998), constitutes an easy and quick way to study genes by reverse genetics. RNAi is particularly effective in *C. elegans* embryos because of the architecture of the oocyte-producing gonad. Double-stranded RNAs (dsRNA) can be conveniently administered by injection, feeding or soaking of worms. Introduction of dsRNA triggers the degradation of the corresponding mRNA in the gonad of the *C. elegans*, while the target protein already existing in the gonad is continually packed into oocytes (Figure 7). As a result, protein levels in newly fertilized embryos gradually decrease between 12 and 48 hours after RNA injection. Importantly, the rate of protein depletion is largely independent of the protein's intrinsic turnover properties, because even proteins with long half-lives are gradually diluted out from the gonad by being packaged into oocytes. This means that embryos gradually more depleted of a specific protein can be readily obtained and gradually more severe phenotypes can be characterized.

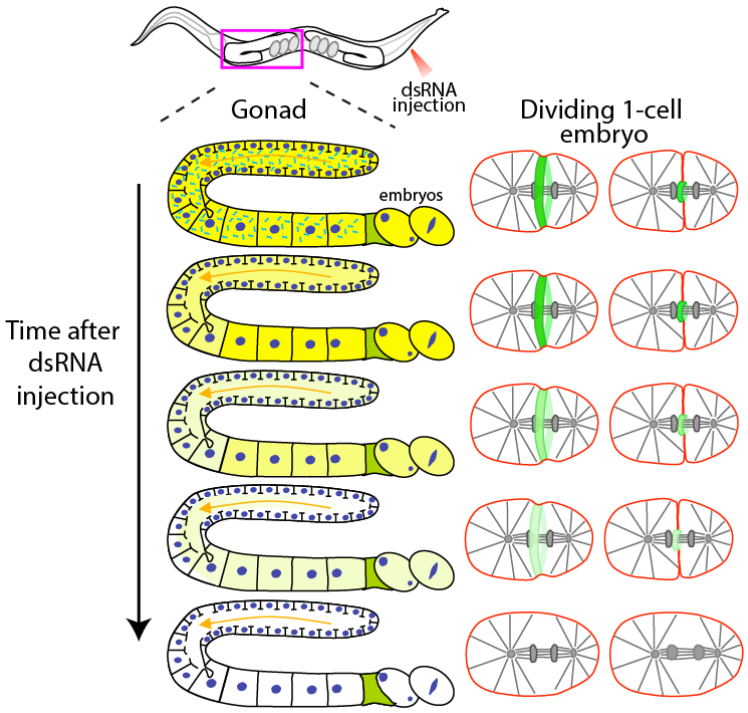

Figure 7 - RNA interference (RNAi) in *C. elegans*. Injection of dsRNA against the gene of interest triggers the degradation of the corresponding mRNA in the gonad**.** Protein levels in newly fertilized embryos gradually decrease between 12 and 48 hours after dsRNA injection.

1.5 Mos Single Copy Insertion

MosSCI - Mos Single Copy Insertion - is a powerful gene manipulation technique that allows the rapid generation of worm strains expressing tagged transgenes at physiological levels. MosSCI allows transgene insertions in a specific chromosomal site in single copy, under the control of the endogenous promoter and 3'-untranslated regions (Figure 8). The worms are injected with a mix of plasmids, one of them carrying the coding sequence of the tagged transgene of interest and another carrying the coding sequence for a transposase. The transposase excises a Mos1 transposon located in a known and defined locus, generating a double strand break. The break is repaired by transferring the DNA from the extrachromosomal template that includes the transgene of interest into the chromosomal site. Positive integration events can be easily screened and final strains will stably express the transgene at endogenous levels in the female and male germline (Frøkjær-jensen et al., 2009). This method is of particular interest when phenotypic analysis of wild-type versus mutant versions of a protein are the basis of a study.

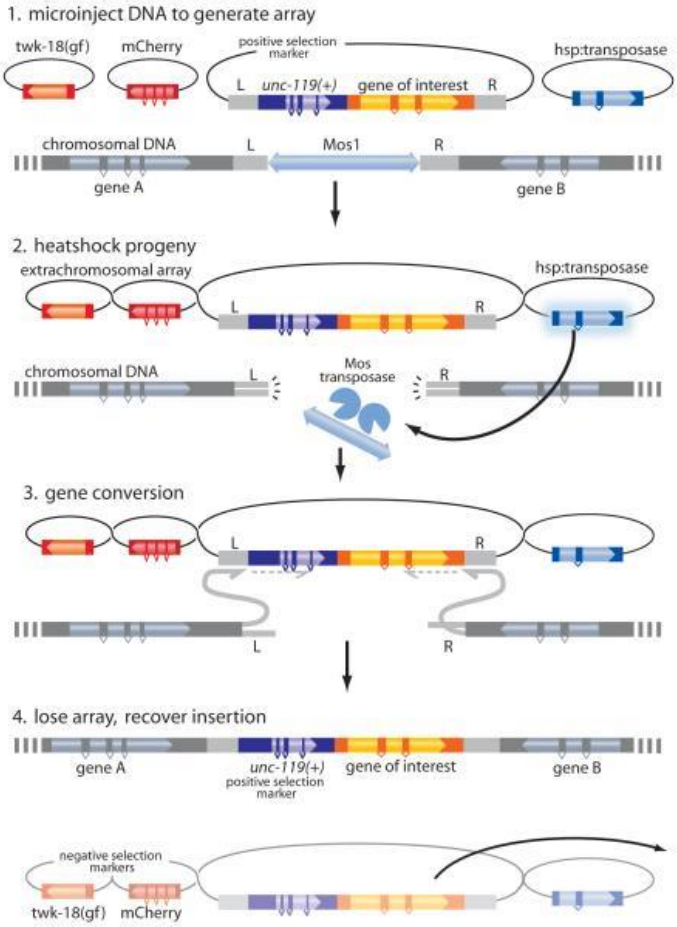

Figure 8 - Schematic representation of the MosSCI methodology. A *mos1* transposon located in a defined locus can be excised by transposase expression resulting in a double-strand break in the chromosome. Presumably the 3′ ends from the left (l) and right (r) flanks invade and anneal to homologous regions in the extrachromosomal array carrying the tagged transgene of interest. The break can then be repaired by synthesis-dependent strand annealing. The positive selection marker *unc-119*(+) and the gene of interest are inserted into the genome by gene conversion. The extrachromosomal array contains a source of transposase (hsp::transposase) and two negative selection markers, twk-18(gf) and fluorescent mCherry markers. *twk-18(gf)* is a temperature-sensitive dominant mutation in a potassium channel, which paralyzes the animals at 25°c. mCherry markers are expressed in the pharynx, body muscle, and nervous system for visual identification of array-carrying animals. (Adapted from Frøkjær-jensen et al., 2009).

2. Objectives

The aim of my work was to understand the role of MRLC phosphorylation during cytokinesis in the *C. elegans* embryo. It is known that MLC-4 (MRLC in *C. elegans*) is essential for cytokinesis (Shelton et al., 1999). However, the functional relevance of MLC-4 phosphorylation on the residues Threonine17 and Serine18 (corresponding to Threonine18 and Serine19 in vertebrates) during cytokinesis requires more thorough studies.

To test the roles of Threonine 17 and Serine 18 phosphorylation of MLC-4 on cytokinesis *in vivo*, we will generate *C. elegans* strains expressing fluorescently tagged non-phosphorylatable Alanine 17 Alanine 18 or phosphomimetic Aspartate 17 Glutamate 18 MLC-4, using MosSCI. To enable functional analysis of the phospho-mutants in the absence of endogenous MLC-4, the transgenes will be engineered to be RNAi resistant. After depletion of endogenous MLC-4 by dsRNA injection, cytokinesis will be evaluated in the 1-cell embryo using quantitative live imaging assays.

This study will be essential to enhance our understanding of NMII regulation/activation and bipolar filament formation during cytokinesis and will contribute to further elucidate the mechanics of contractile ring constriction.

3. Material and Methods

3.1. C. elegans maintenance

3.1.1 Worm maintenance

C. elegans strains were grown on a monoxenic culture using E. coli OP50 strain as food source (Brenner, 1974). An initial culture of E. coli OP50 was obtained by streaking out some bacteria from a glycerol stock onto a LB agar plate [10 g/L Bacto-tryptone, 5 g/L Bacto-yeast, 5 g/L NaCl and 15 g/L agar, pH 7.5]. Bacteria colonies were left to grow overnight at 37ºC (Byerly et al., 1976). A single colony of OP50 was inoculated on LB liquid medium and grown overnight at 37 ºC. The bacterial suspension was used for seeding NGM plates.

C. elegans strains were maintained on Nematode Growth Medium (NGM) agar (Brenner, 1974). Medium size plates (60 mm diameter) were used for general strain maintenance, and larger plates (100 mm diameter) were used for growing larger quantities of worms for freezing. NGM [3 g/L NaCl, 17 g/L agar and 2.5 g/L peptone] was sterilized by autoclaving at 110ºC for 30 minutes. After cooling 1M $CaCl_2$, 5mg/ml cholesterol in ethanol, 100 mM $MgSO_4$ and 100 mM KPO_4 were added. Using sterile procedures, NGM solution was dispensed into plates using a peristaltic pump (Wheaton Science Products). This pump was adjusted in order to dispense a constant amount of NGM agar into each plate. Plates were left to dry at room temperature for 2-3 days before. Plates were then seeded with 0.05 ml of E. coli OP50 liquid culture for medium NGM plates or 0.1 ml for large NGM plates and left at room temperature for one day before storage.

3.1.1. General stock maintenance

C. elegans stocks were maintained between 16°C and 25°C, most typically at 20°C. This variation in temperature periods was useful when planning experiments. Every plate had on the bottom the strain name identification and date. Occasionally, *C. elegans* stocks became contaminated and a standard alkaline bleach protocol was used to clean the worms up (Eisenmann, 2005). The bleach kills the contaminants and hermaphrodites but soaks onto the plate before the embryos hatch. The next day the larvae crawl onto the E. coli OP50 lawn and are transferred to a clean seeded NGM plate.

3.1.2. Freezing C. elegans stocks

15 young adults were picked onto each of two 10 cm plates seeded with OP50 and grown until the food lawn had just been depleted. At this point, plates should have plenty of L1s worms, which are best suited to withstand freezing. Plates were rinsed twice with 5mL S-Basal [100nM NaCl, 50mM K_2HPO_4 (pH 6.0), 5000 mg cholesterol] to loosen worms that were stuck to the agar and collected in a 15 mL conical tube. The worms were spun down for about 1 minute (speed?) in a clinical centrifuge, and washed twice with 15mL S-basal. After the second wash the supernatant was removed leaving 2.5mL S-basal and mixed with an equal amount of freezing medium [100mM NaCl, 50mM KH_2PO_4 (pH 6.0), 30 % (v/v) glycerol]. Worms were re-suspended and aliquoted in cryovials (1 mL of worm suspension per cryovial) and then stored at -80ºC in a Coolcell container to allow for gradual decrease of temperature.

3.2. Generation of C. elegans strains

3.2.1. Design and cloning of transgenes

MLC4(T17S18AA)::GFP and MLC4(T17S18DE)::GFP mutant transgenes were made by mutating the desired residues in a vector carrying a fragment of mlc-4-GFP (8558 bp, Figure 11). Mutagenesis was carried out by using overlap extension PCR with appropriate primers as shown in figure 9 (Heckman, KL & Pease LR, 2007). Initial PCRs using primers a+c and b+d (Table 1) generated overlapping gene segments that were then used as template DNA for another PCR using primers a and d (Table 1). Internal primers b and c correspond to overlapping, complementary sequences and contain nucleotide substitutions. Overlapping strands of products AC, BD hybridize and are extended to generate the full-length product amplified by the flanking primers a and d. Primers a and d include restriction enzyme sites for inserting the final product into an expression vector for cloning purposes.

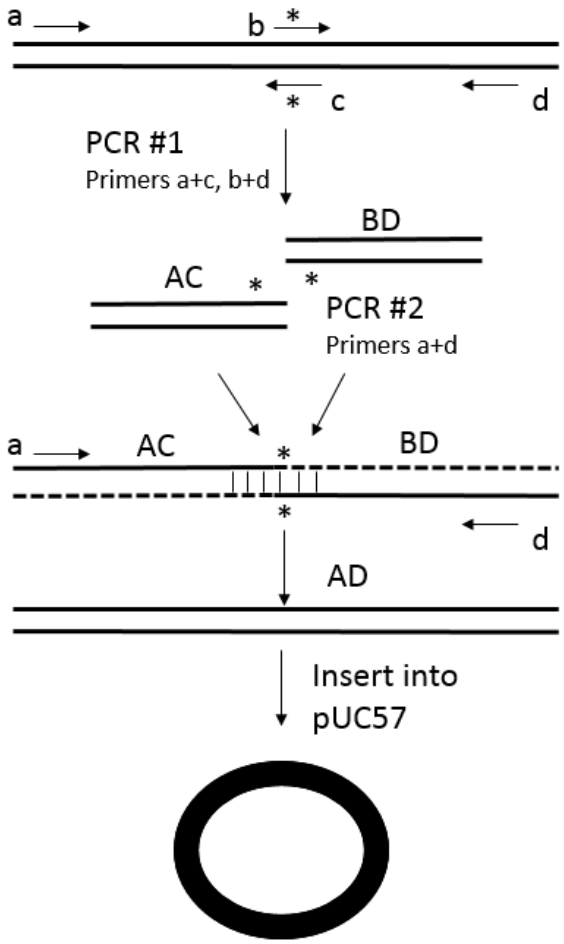

Figure 9 - Site-direct mutagenesis by overlap extension PCR method used to create *mlc-4* mutant transgenes. Using mutagenic primers (b and c) and flanking primers (a and d), intermediate PCR products (AC and BD) were generated. These PCR products have overlapping fragments carrying the mutations that allow for the generation of the final PCR product (AD). As flanking primers had EcoNI and MluI restriction enzyme recognition sites it was possible to insert the final PCR product in the pUC57 intermediate vector.

.

Table 1 - Primers and PCR conditions used on overlap extension PCR method. Primers a and d include enzymatic restriction sites that allow for the insertion of the final PCR product in pUC57. Primers b and c include mutations on threonine17 and serine18 aminoacids to generate MLC-4 T17S18AA::GFP and MLC-4 T17S18DE::GFP transgenes (b1+c1 and b2+c2, respectively). Phusion DNA polymerase was used.

Forward primer sequence a	5'ccccctttccaaggcgacaaacgc 3'	
Reverse primer sequence b1	3'gcgaatacgttggcggcagcgcgttgcgg5'	
Reverse primer sequence b2	3'gcgaatacgttctcgtcagcgcgttgcgg5'	
Forward primer sequence c1	5'ccgcaacgcgctgccgccaacgtattcgc 3'	
Forward primer sequence c2	5'ccgcaacgcgctgacgagaacgtattcgc 3'	
Reverse primer sequence d	3'ctttactcatctgcagacctccagcctcatccttg5'	
PCR conditions		
Temperature	***Time***	
98 ºC	***30 seconds***	
98 ºC	***10 seconds***	***×30 cycles***
58 ºC	***20 seconds/kb***	
72 ºC	***35 seconds***	
4 ºC	***hold***	

In order to purify the *mlc-4* amplified band from 1% agarose gel, the NucleoSpin kit (Macherey-Nagel) was used according to manufacturer's instructions. Both MLC-4 mutant transgenes were first cloned into the intermediate vector *p*UC57 (Figure 10).

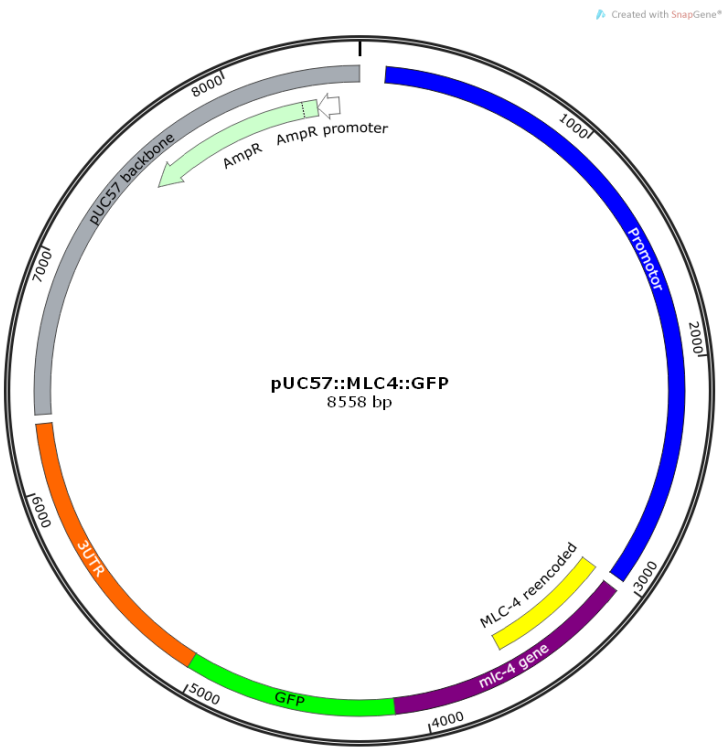

Figure 10 - Map of pUC57- MLC-4(reencoded)::GFP. pUC57 was used as intermediate plasmid in cloning strategy. Map was generated by Snapgene software.

The pUC57 intermediate vector and *mlc-4* product previously obtained were cut with *EcoNI and MluI* enzymes *(NEB),* at 37 ºC for 3 hrs. To prevent vector re-ligation Calf Intestinal Phosphatase (CIP) was added. After enzymatic digestion, the products were run on 1% agarose gel in order to purify the bands of interest (empty pUC57 vector: 6858 bp and mutant inserts 1718 bp) using NucleoSpin kit (Macherey-Nagel). For ligation of the mutants *mlc-4* and the empty pUC57, a 1:6 molar ratio of insert:vector was used. T4 DNA ligase was the enzyme used (Thermo Scientific). The ligation reaction was incubated at 16 °C for 2 hrs. The ligation reaction was added to competent DH5α cells (100 µL) and incubated on ice for 15 min. Cells were heat-shocked at 42 °C for 1 min and placed on ice for 2 min to cool. As the plasmid confers ampicillin resistance, cells were directly plated on LB plates with Ampicilin antibiotic. Plates were incubated over-night at 37ºC for colony growth. To confirm that cloning occurred as expected, 6 single colonies were transferred into liquid LB with ampicillin. Cultures were grown overnight at 37 °C and the plasmids purified using the NucleoSpin Plasmid Mini Prep Kit (Macherey-Nagel) from 4 mL of bacterial culture. Diagnosis using restriction enzymes was performed and positive plasmids were sequenced by GATC (represented in Portugal by NZYtech). The final phase of cloning consisted

in transferring the transgenes to the final vector, *pCFJ151,* 13539 bp (Figure 11). Transfer was done by cutting mutated versions of *mlc-4* from pUC57 with *SpeI* restriction enzyme (NEB) and ligating it to SpeI-cut pCFJ151. pCFJ151 plasmid contains two homology sequences for insertion of our transgene in the ttTi5605 locus of chromosome II, in the strain EG6699. It also contains the sequence for the *unc-119* gene, which is essential for screening of strains where integration has occurred.

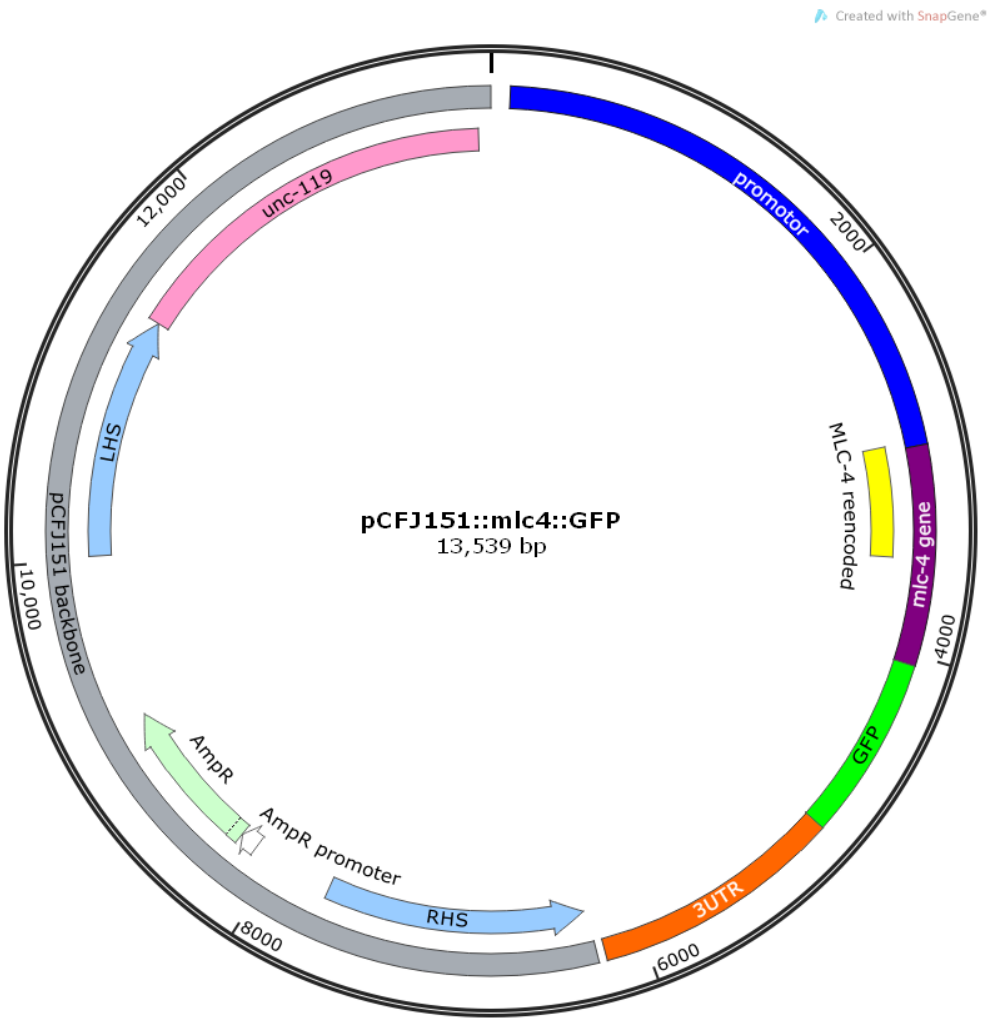

Figure 11 - Map of pCFJ151::MLC-4::GFP. pCFJ151 was used as final plasmid. This is the standard plasmid used in MosSCI for integration in the chromosome II. It contains an ampicillin resistance gene (AmpR) that allows for MLC-4::GFP transformed bacteria growth on selective medium containing ampicillin; Left and Right Homology sequences that allow for integration into *ttti5605 locus* in chromosome II (LHS and RHS); our transgene MLC-4 mutant, and an *unc-119* that is a positive selection marker. Map was generated by Snapgene software.

3.2.2. Stable integration using MosSCI technique

All strains used (except strain expressing H2B::mCherry, which was created by bombardment) were generated by Mos1-mediated single copy (MosSCI) described in the introduction section 7. MosSCI allows that a single copy of the transgene of interest is inserted in a defined chromosomal locus. A mix of plasmids, one of which carries the transgene of interest and the *unc-119* gene is injected in the worm germline. Genome integration of the transgene is identified in the F2 progeny based on ability to move (worms initially injected are immobile and *unc-119* expression makes them move normally), survival in heat-shock conditions and absence of fluorescent co-injection markers. Original strain used for MosSCI integrations in chromosome II (EG6999) was maintained on HB101 bacteria at 16 ºC. Young adult hermaphrodites were injected with injection mix (Table 2) on a Zeiss Axiovert S100 coupled to a microinjection setup consisting of a PatchMan NP2 and FemtoJet Express (Eppendorf).

Table 2 MosSCI injection mix. Plasmid mix used to generate worm strains by MosSCI that is composed of plasmids carrying several fluorescent co-injection markers (pMA122, pGH8, pCFJ90, and pCFJ104), our targeting vector (pCFJ151::MLC-4::GFP) and a plasmid that encodes for the transposase responsible for integration (pCFJ601). DNA ladder was added to the mix to achieve the ideal injection mix concentration.

Plasmid	Description	Final concentration
pCFJ601	**Peft-3::transposase**	**50 ng/µl**
Transgene in pCFJ151	***mlc-4* mutants (T17S18AA/T17S18DE)**	**10 - 50 ng/µl**
pMA122	**Phsp::peel-1**	**10 ng/µl**
pGH8	**Prab-3::mCherry (Pan-neuronal)**	**10 ng/µl**
pCFJ90	**Pmyo-2::mCherry (pharynx muscle)**	**2.5 ng/µl**
pCFJ104	**Pmyo-3::mCherry (body muscle)**	**5 ng/µl**
	DNA ladder	**Add to 100 ng/µl**

Injected worms were placed on plates at 20 ºC and left to recover for approximately one hour. The plates were transferred to 25 ºC until worms starved. Worms were then heat-shocked at 34°C for 4h and left at 25 ºC overnight. In the following day, the worms were screened for MosSCI insertions on a fluorescence dissection stereoscope (Nikon, SMZ1000 equipped with

Intensilight). Animals where integration events occurred moved well, did not have any of the fluorescent co-injection markers (mCherry signal) and expressed MLC-4::GFP. Genomic DNA of worms expressing MLC4(T17S18AA)::GFP and MLC4(T17S18DE)::GFP was extracted using Quiagen extraction kit according to manufactory's instructions. Long-range PCR was carried out to confirm correct transgene integration.

Table 3 – Primers and PCR conditions to check for correct integration of *mlc-4* in Chromosome II.

Reverse primer sequence a	5’ gacatttgagaatggcattga 3’	
Forward primer sequence b	3’ cgaagatctgcccactagtaacaagggaagcagtgttc 5’	
Forward primer sequence c	5’ gttttacgggatgccatggcttactgc 3’	
Reverse primer sequence d	3’ atcgggaggcgaacctaactg 5’	
PCR conditions		
Temperature	***Time***	
98 ºC	***30 seconds***	
98 ºC	***10 seconds***	***×30 cycles***
58 ºC	***1 minute /kb***	
72 ºC	***35 seconds***	
4 ºC	***hold***	

3.2.3. Mating strains

Strains expressing MLC-4 phospho-mutants were crossed with another *C. elegans* strain expressing H2B::mCherry, a chromosome marker. As previous described, strains expressing mutant MLC-4::GFP were created by MosSCI technique. GFP was crucial for protein localization studies and for quantification purposes. The H2B::mCherry marker was useful to determine anaphase onset, the time reference used. For strain crossing, males expressing H2B::mCherry were generated by heat-shock. Plates were placed on an incubator at 34 ºC for 4 hours and then transferred to 20 ºC. Progeny was screened for males. Male worms were easy to distinguish because of the visible copulatory apparatus at the end of the tail (Figure 12).Then, 12 males expressing H2B::mCherry and 6 hermaphrodites expressing MLC-4::GFP mutant were let to mate at 20 ºC for 24 hours. Hermaphrodites were singled out and the progeny of worms that had successfully mated was 50% males. All progeny of mated worms should be heterozygous for both H2B::mCherry and MLC-4::GFP mutant.

The progeny of the heterozygous worms (F2) can carry zero, one or two copies of either marker MLC-4::GFP and H2B::mCherry. Homozygous worms for both MLC-4::GFP and H2B::mCherry were isolated over the following three generations.

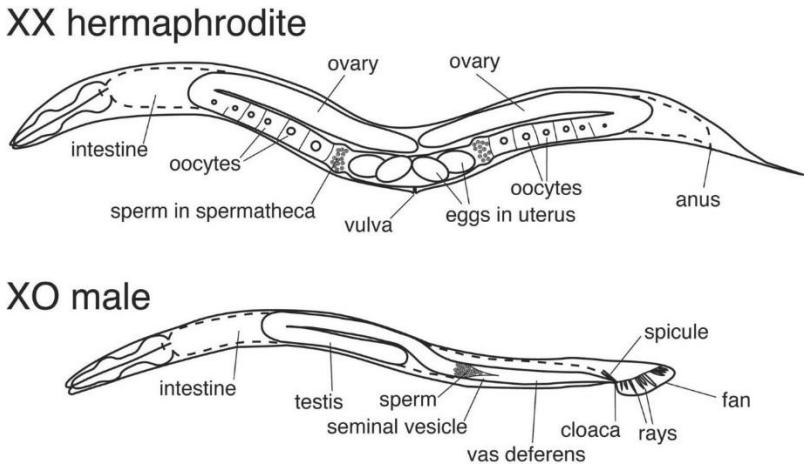

Figure 12 - Hermaphrodite and male *C. elegans* representation. The hermaphrodite adult (XX) has different sexual organs from the male (XO). The presence of a copulatory organ on the male tail distinguishes males from hermaphrodites. (Adapted from: David zarkower,2006)

3.2.4. Strains generated during this project

In order to characterize the role of phosphorylation of the residues Threonine 17 and Serine 18 in MLC-4 during cytokinesis, the strains listed in table 4 were used.

Table 4 - *C. elegans* strains used in this study. GCP110 and GCP112 correspond to strains expressing MLC-4 non-phosphorylatable and phosphomimetic form, respectively, that were generated for the purpose of this study. The other strains already existed in our laboratory.

Strain	Strain name	Genotype
OD56	**H2B::mCherry**	unc-119(ed3)III; ltIs37[pAC64; Ppie-1::mCherry::his-58; unc-119(+)]IV
GCP9	**NMY2::GFP H2B::mCherry**	unc-119(ed3)III; prtSi8[pAC95; Pnmy-2::nmy-2reencoded::GFP::StrepTagII::3'UTRnmy-2; cb-unc-119(+)]II; unc-119(ed3) III; ltIs37 [pAC64; Ppie-1::mCherry::his-58]IV

GCP16	**MLC4::GFP**	unc-119(ed3)III; prtSi4[pAC72; Pmlc-4::mlc-4 reencoded::GFP::StrepTagII::3'UTRmlc-4; cb-unc-119(+)]II
GCP50	**MLC4::GFP H2B::mCherry**	unc-119(ed3)III; prtSi4[pAC72; Pmlc-4::mlc-4 reencoded::GFP::StrepTagII::3'UTRmlc-4; cb-unc-119(+)]II; ltIs37 [pAA64; pie-1::mCherry::his-58; unc-119 (+)] IV
GCP110	**MLC4(T17S18AA)::GFP**	unc-119(ed3)III; prtSi4[pAC72; Pmlc-4::mlc-4 (T17A;S18A)reencoded::GFP::StrepTagII::3'UTRmlc-4; cb-unc-119(+)]II
GCP112	**MLC4 (T17S18DE)::GFP**	unc-119(ed3)III; prtSi4[pAC72; Pmlc-4::mlc-4 (T17D;S18E)reencoded::GFP::StrepTagII::3'UTRmlc-4; cb-unc-119(+)]II

GCP9 strain was used as a control for our quantitative live imaging assays and to characterize endogenous MLC-4 depletion.

3.3. RNA interference

Fire and Mello discovered that injection of double stranded RNA (dsRNA) into worms leads to specific degradation of the corresponding mRNA, a process termed RNA interference (RNAi) (Fire et al., 1998). Subsequently, it was found that either soaking worms in dsRNA solution or feeding worms bacteria engineered to produce dsRNA also could induce a robust RNAi response (Tabara et al., 1998; Timmons and Fire, 1998). RNAi by injection was used in this project. dsRNA was produced as previously described (Oegema et al., 2001) and injected into L4 stage hermaphrodites. Depleted embryos were characterized by spinning-disk confocal live imaging. Since the MLC-4 transgenes we made are RNAi resistant, it is possible to delete the endogenous protein and characterize phenotypes in the presence of the mutant forms only (Figure 13).

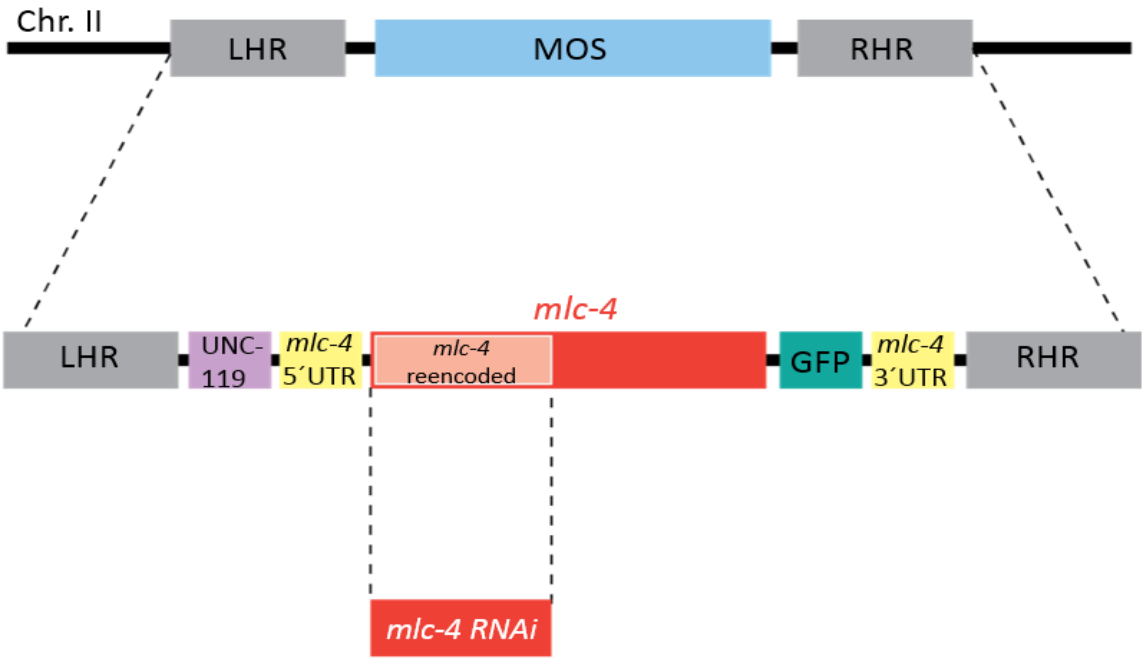

Figure 13 - Schematic representation of the mlc-4 transgene after correct insertion in the ttTi5605 locus on Chromosome II. Left and right homology regions flank the transgene. Integrated sequence includes the unc-119 gene that permits worm movement and the mlc-4 gene under the endogenous promoter and 3´UTR. The mlc-4 coding sequence has a re-encoded region of 562 base pairs that although still coding for the same aminoacids, it is different from the corresponding sequence in the endogenous gene. Depletion of endogenous MLC-4 and not exogenous MLC-4 can be achieved with a dsRNA that targets only that region in the endogenous gene.

In order to produce *mlc-4* dsRNA, a 638 bp portion of the *mlc-4* gene was amplified from *C. elegans* wild-type N2 genomic DNA using the primers and PCR conditions on Table 5.

Table 5: Primers and PCR conditions used to amplify the template *for mlc-4 dsRNA production. Phusion DNA polymerase was used.*

Forward primer sequence	5’ aattaaccctcactaaag gctcccgcaaaaccgtaaac 3’	
Reverse primer sequence	3’ taatacgactcactatagg cttaatcggagcatctctaaag 5’	
PCR conditions		
Temperature	***Time***	
98 ºC	***30 seconds***	
98 ºC	***10 seconds***	***×30 cycles***
58 ºC	***20 seconds/kb***	
72 ºC	***35 seconds***	
4 ºC	***Hold***	

PCR template was purified with the NZYTech PCR clean-up kit eluted on 33 µL of DNA Elution Buffer and quantified with the Nanodrop. For T3 transcription reaction, the Ambion Megascript kit was used and for T7, the NEB T7 High Yield RNA Synthesis kit was used. The protocol described was the same for both kits (Table 6).

Table 6: Reagents for transcription of DNA into RNA.

Reagents mix
10 µL rNTP mix
2.5 µL 10 x T3 or T7 buffer
10 µL *mlc-4* PCR DNA template (**~ 1µg total**)
2.5 µL T3 or T7 enzyme mix

Transcription reactions were assembled at room temperature and components were added in the order on table 6 and incubated at 37 °C for 5 hours. To infer if transcription occurred correctly 1 µL of each reaction was run on a 1% agarose gel. Degradation of DNA template was done by adding 1 µL of DNase (from the Megascript kit) to each reaction and incubated at 37 °C for 15 minutes. The transcript was purified using the Megaclear kit and eluted in 33 µL. 1 µL of the T3 and T7 reactions were run on 1% agarose gel in RNAse free conditions. T3 RNA reaction, T7 RNA reaction and 3x Soaking Buffer (6.3mM NaCl, 14.1mM NH_4Cl, 32.7mM Na_2HPO_4, 16.5 mM KH_2PO_4) were combined on a 1:1:1 ratio. The solution was incubated at 68 °C for 10 min and then at 37 °C for 30 minutes to anneal. The efficiency of annealing was tested by running 1 µL of the annealed sample on a 1% TAE agarose gel. dsRNA concentration was measured on Nanodrop

3.4. Embryonic Viability test

The embryonic viability test was performed to check whether depletion of endogenous mlc-4 led to embryonic lethality. The test was followed as depicted in Figure 14.

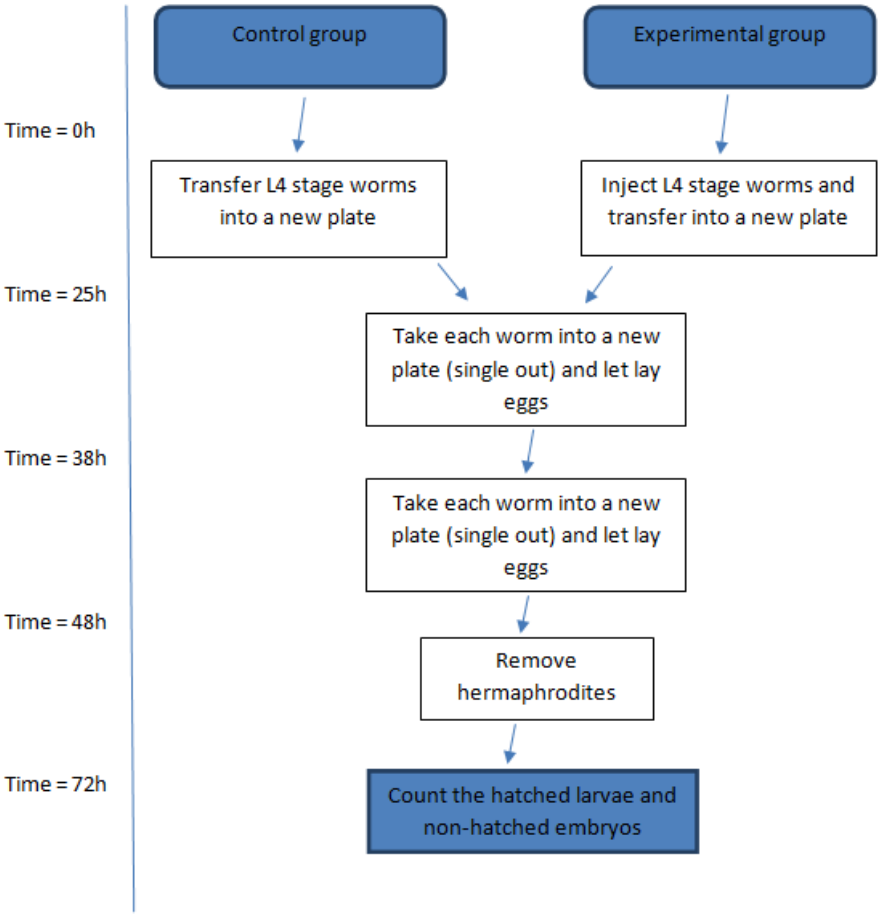

Figure 14 - Schematic representation of Embryonic Viability Test experiment. Single L4 stage worms injected or not with dsRNA against endogenous *mlc-4* were sequentially transferred to fresh plates 25 hours and 38 hours post-injection. 48h hours post-injection, the mother was removed. The day after, all embryos that had been laid should have hatched if viable. Hatched larvae and dead embryos were counted.

3.5. Microscopy

3.5.1. *Preparation of samples*

Gravid hermaphrodites were dissected and early embryos were mounted on 2% agarose pads and covered with 18 × 18 mm coverslips in M9 medium (Brenner, 1974).

3.5.2. RNImaging conditions

Embryos were imaged at 20 °C using an epifluorescence microscope (Zeiss Axiobserver Z1) equipped with DIC optics, a 63× Plan-Apochromat lens (0.55 NA). Acquisition parameters, shutters, and focus were controlled by Zen software (Zeiss). Images of MLC-4::GFP were taken by acquiring five z-planes 1 µm apart, every 10 seconds through the centre of the embryo using an Orca 4.0 flash camera (Hamamatsu). Images of mCherry labeled histone H2B and DIC were taken by acquiring one z-plane every 10 seconds in the centre of the embryo. Exposure times were 50 miliseconds for both GFP and mCherry channels (554 nm and 625 nm LEDs (Colibri 2) used at 30% and 25% of the maximum power, respectively).

3.5.3. Imaging processing

Microscopy images were processed and analysed with ImageJ software. To enable visual comparisons, the GFP signal of different images was scaled. Best focused z-plane per time point was chosen for figure display. Graphs were built with GraphPrism software.

3.6. Live-imaging assays

3.6.1. Measuring Timing for Contractile Ring Assembly

Interval A is the time between anaphase onset and cortical shallow deformation at the equator of the cell. Interval B is the time between cortical shallow deformation and back-to-back membrane formation. Anaphase onset was the time at which the separation of the two chromosome masses was observed as judged by H2B-mCherry signal. Time of shallow deformation corresponded to the first frame where a deformation is observed at the equator of the cell as judged by the MLC-4::GFP signal. Time of back-to-back membrane formation corresponded to the first frame where two juxtaposed plasma membranes were observed as judged by the MLC-4::GFP signal.

3.6.2. Measuring Contractile Ring rate

The diameter of the contractile ring was measured in the section that showed a maximum distance between the two sides of the furrow at each time point. Individual traces of furrow diameter versus time were plotted and averaged.

4. Results

4.1. MLC-4 gradual depletion in one-cell *C. elegans* embryos results in cytokinesis slow-down, cytokinesis failure and worm sterility

Myosin regulatory light chain (MLC-4 in *C. elegans*) was previously shown to be essential for cytokinesis in *C. elegans* embryos since depletion by RNAi resulted in cytokinesis failure and embryonic lethality (Shelton, 1999). To better understand the role of MLC-4 in cytokinesis, we used a strain expressing non-muscle myosin II heavy chain labelled with GFP (NMY-2::GFP) as a contractile ring reporter and the first embryonic division as model. Our lab has established assays to evaluate contractile ring performance at this cell stage (Figure 1): 1) evaluation of ring assembly by measuring interval A - from anaphase to shallow deformation of the membrane that corresponds to the mobilization of ring components to the cell equator, and interval B - from shallow deformation to back-to-back plasma membrane that corresponds to ring maturation and beginning of constriction; 2) evaluation of contractile ring constriction by measuring the distance between the two furrow tips as the ring gets smaller.

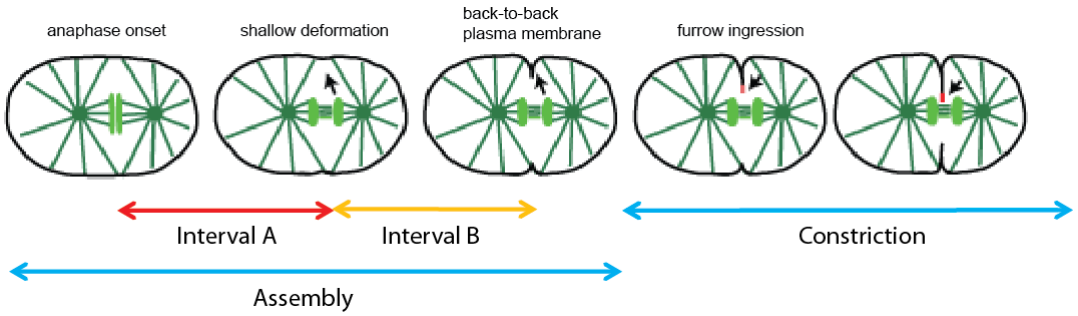

Figure 1 - Schematic diagram illustrating contractile ring assembly and constriction phases during cytokinesis in the one-cell embryo. Contractile ring assembly was followed by measuring interval A - from anaphase onset to shallow deformation, and interval B - from shallow deformation to back-to-back plasma membrane; contractile ring constriction was evaluated by measuring the distance between the two furrow tips during ring closure. Arrows indicate in order: cortical shallow deformation, back-to-back plasma membrane configuration and accumulation of contractile ring proteins (red) at the tip of the furrow.

To evaluate the best depletion level for our analysis, we did an RNAi time course experiment (introduction section 3.3) to gradually reduce MLC-4 levels in embryos and assess its effects in embryonic viability. Worms became sterile and stopped laying eggs 38 hours post dsRNA injection at 20ºC. We reduced depletion levels by analyzing embryos laid between 25 and

38 hours post-injection. At this time frame, the worms were able to lay eggs but none of these were viable, when compared to non-injected control embryos that were 100% viable. We therefore chose to image one-cell embryos during this window of time. MLC-4 depleted embryos failed cytokinesis 25 hours post-injection whereas cytokinesis completed in non-depleted embryos (Figure 2, movie 1 in the middle). This severe phenotype did not allow us to determine the precise roles of MLC-4 during cytokinesis. We looked at earlier time points to reduce depletion levels and found that at 23 hours post-injection all embryos were still able to complete cytokinesis (Figure 2 and 3, movie 1 in the right).

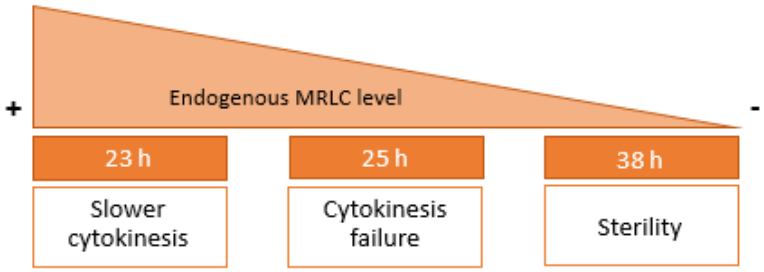

Figure 2 - Phenotypic characterization of embryos progressively depleted of MLC-4. Worms expressing NMY2::GFP were injected with dsRNA against *mlc-4*. One-cell embryos laid at different windows of time after dsRNA injection, were analyzed. At 23 hours post-injection, embryos divided slower. At 25 hours post-injection, embryos failed cytokinesis. At 38 hours post-injection, there were no more embryos to be analyzed because the worms had become sterile.

We measured contractile ring assembly and constriction parameters from movies of injected and non-injected embryos at this time point. In control cells, interval A had an average value of 60s and was increased to 300s in MLC-4 depleted embryos. Similarly, interval B that averaged 40s in controls was increased almost four-fold to an average of 150s in depleted embryos (Figure 3B-C). These results indicate that the depletion of MLC-4 has a strong impact on the assembly of the contractile ring. Control embryos completed cytokinesis in approximately 240s after anaphase onset whereas MLC-4 depleted embryos took in average 650s to complete cytokinesis. Additionally, MLC-4 depleted embryos showed a clear slowdown at the last stages of constriction indicating possible abscission problems (Figure 3D-E). We calculated ring constriction rate by linear regression in the 25 µm to 15 µm diameter interval. The average rate of constriction was of 0.16 µm/s in control embryos and 0.09 µm/s in MLC-4 depleted embryos. Together these results suggest that MLC-4 partial depletion strongly delays cytokinesis by affecting both the assembly and constriction of the contractile ring.

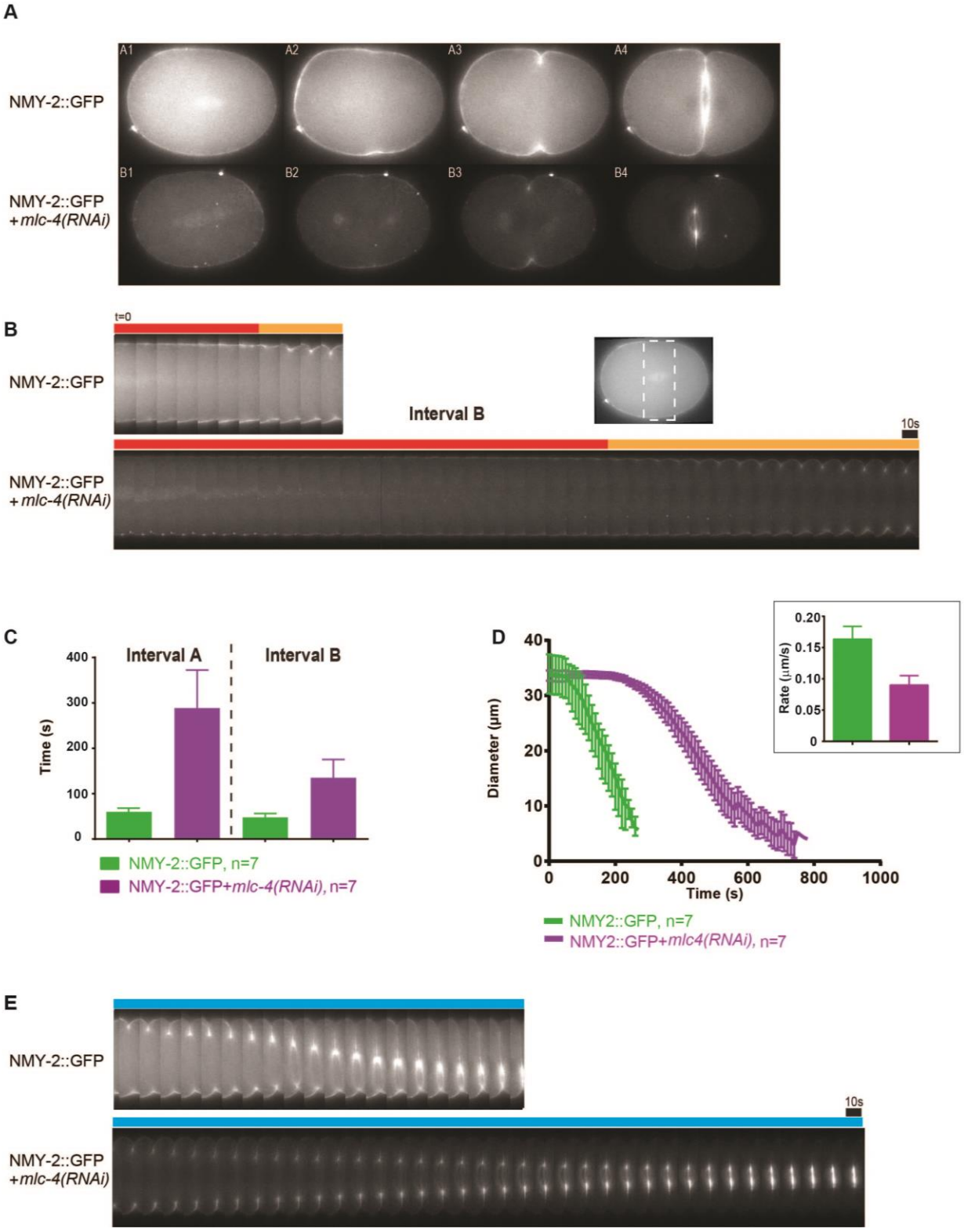

Figure 3 - MLC-4 partial depletion leads to cytokinesis slow-down and failure. (A) Worms expressing NMY2::GFP were injected with dsRNA against mlc-4 and contractile ring assembly and constriction were followed in one-cell

embryos at 23-25h post-injection, time point at which the embryos were still able to complete cytokinesis. (B) Representative montages of the furrow region during contractile ring assembly for embryos expressing NMY2::GFP that had been depleted or not of MLC-4; red bar and orange bar represent interval A and interval B, respectively. Scale bar, 10s. (C) Contractile ring assembly was evaluated by measuring intervals A and B for embryos expressing NMY2::GFP in the presence (green) or absence of endogenous MLC-4 (purple). (D) Mean contractile ring diameter is plotted versus time for embryos expressing NMY2::GFP in the presence (green) or absence of MLC-4 (purple). Each curve represents the average of embryos (n=7). Time zero corresponds to anaphase onset. Mean of constriction rate (µm/s) is shown for each group (inset graph). (E) Representative montages of the furrow region during contractile ring constriction (blue bars) for embryos expressing NMY2::GFP in the presence or absence of MLC-4. Scale bar, 10s Error bars are 95% confidence intervals.

NMY-2 and MLC-4 are expected to co-localize throughout cytokinesis as they exist in a protein complex (introduction section 1.2). To investigate the localization relationship between NMY-2 and MLC-4 in the one-cell embryo during cytokinesis, imaging of embryos expressing transgenic NMY-2::GFP or MLC-4::GFP was performed. As shown in Figure 4, panels A and B, NMY-2::GFP localized in the cytoplasm and at the spindle at the time of anaphase onset (A1), at the equatorial cortical region during shallow deformation (A2), at the furrow (A3) and in the contractile ring (tip of the furrow, A4). When MLC-4 was partially depleted, the localization of NMY-2::GFP was similar (Figure 4B), but the signal intensity was weaker, the spindle signal persisted for longer and aggregates were visible in the cytoplasm (A1-A4 panels were compared with panels B1-B4; aggregates are shown in orange boxes As expected, MLC-4::GFP was found to localize identically to NMY-2::GFP in the presence (panels C1-C4) or absence (panels D1-D4) of endogenous MLC-4. However, MLC-4::GFP signal intensity increased in embryos depleted for endogenous protein.

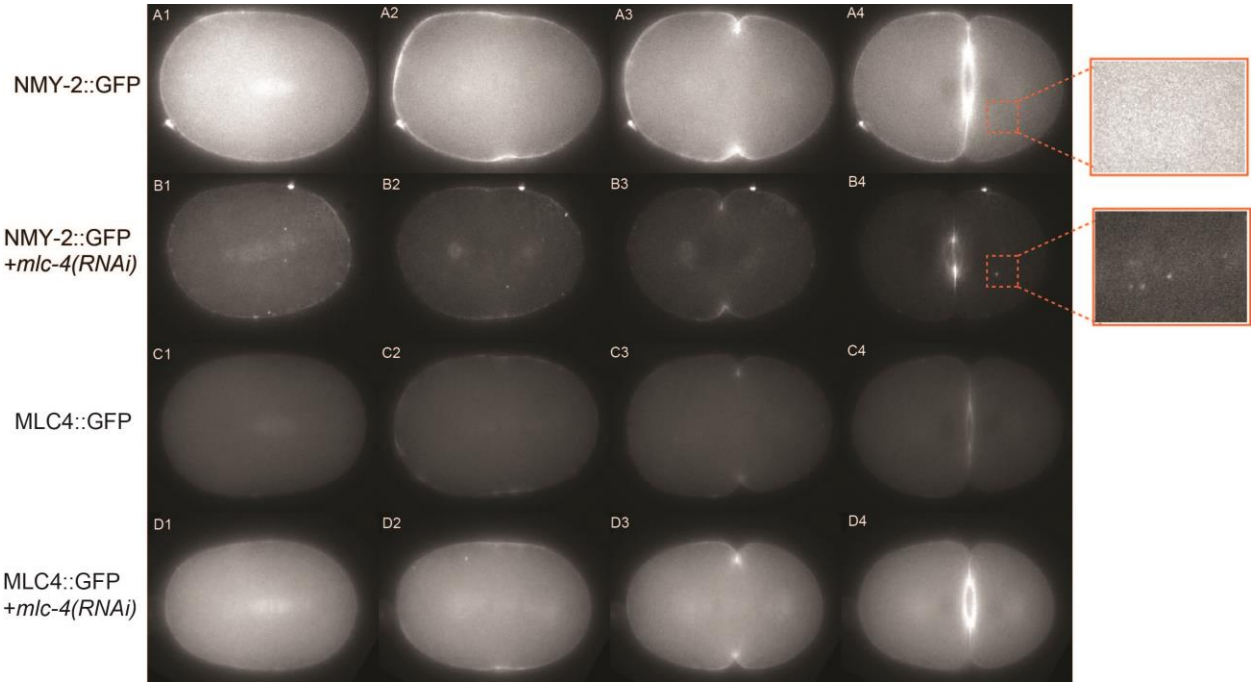

Figure 4 – Localization of NMY-2::GFP and MLC-4::GFP in one-cell embryos during cytokinesis in the presence or absence of endogenous MLC-4. NMY-2::GFP localizes in the cytoplasm and mitotic spindle (A1,B1), accumulates on the cortical equatorial region (A2,B2), at the furrow (A3,B3), and in the contractile ring (A4,B4) in both control embryos (panels A) and MLC-4 depleted embryos (panels B). MLC-4 depleted embryos show however, reduced NMY2::GFP signal and protein aggregates (orange boxes with different scaling). MLC-4::GFP (panels C and D) localizes as NMY-2::GFP (panels A and B) when endogenous MLC-4 is present (C1-C4) or absent (D1-D4). Mlc-4 depleted embryos show however, increased levels of MLC-4::GFP.

4.2. Wild-Type MLC-4::GFP probe is functional

To study the regulation by phosphorylation of MLC-4 during cytokinesis, we started by generating a worm strain expressing a fluorescent tagged version of wild-type MLC-4 (MLC-4::GFP, Figure 4 panels C and D). We injected worm gonads with a vector containing the full length MLC-4 genomic locus tagged with GFP at the C-terminus and containing endogenous promoter (2.85 kb) and 3'UTR (1.3 kb) regions. For RNAi resistance the region 4-566 bp was re-encoded by using alternative codons while maintaining protein sequence. This allows us to specifically deplete the endogenous gene by using a dsRNA that targets the sequence 4-566 bp in the endogenous gene (dsRNA-endog). We obtained a viable strain and the genomic integration was confirmed by PCR amplification with specific primers. To evaluate if the transgene was capable of functionally replacing the endogenous protein, we performed embryonic viability tests on embryos laid between 44 and 48h after dsRNA injection against endogenous mlc-4. Wild-type worms (N2 strain) injected with the dsRNA against endogenous mlc-4 did not hatch. As mentioned in section 4.1, no embryos expressing NMY-2::GFP hatched when MLC-4 was depleted. In contrast, embryos expressing transgenic MLC-4::GFP were 100% viable, indicating that the transgene is functional and able to fully rescue the depletion of the endogenous protein. To examine the behavior of MLC-4::GFP expressing embryos in the presence and absence of endogenous protein, we imaged them to assess protein localization (figure 4 panels C,D), protein intensity levels and cytokinesis kinetics (movie 2). MLC-4::GFP localization was the same in both cases, except that the levels in the contractile ring are higher in the absence of endogenous protein (Figure 4C,D). Intervals A (t = 60s) and B (t=40s) were similar in both cases (Figure 5B,E). The ring constriction profile was also similar in both cases: it took 250s in average to complete cytokinesis (Figure 5E,D) and similar results were obtained for ring constriction rates: 0.16 µm/s (Figure 5C). This constriction rate was identical to that measured in embryos expressing NMY-2::GFP (Figure 3D). These results strongly suggest that the transgenic MLC-4::GFP performs identically to the endogenous MLC-4.

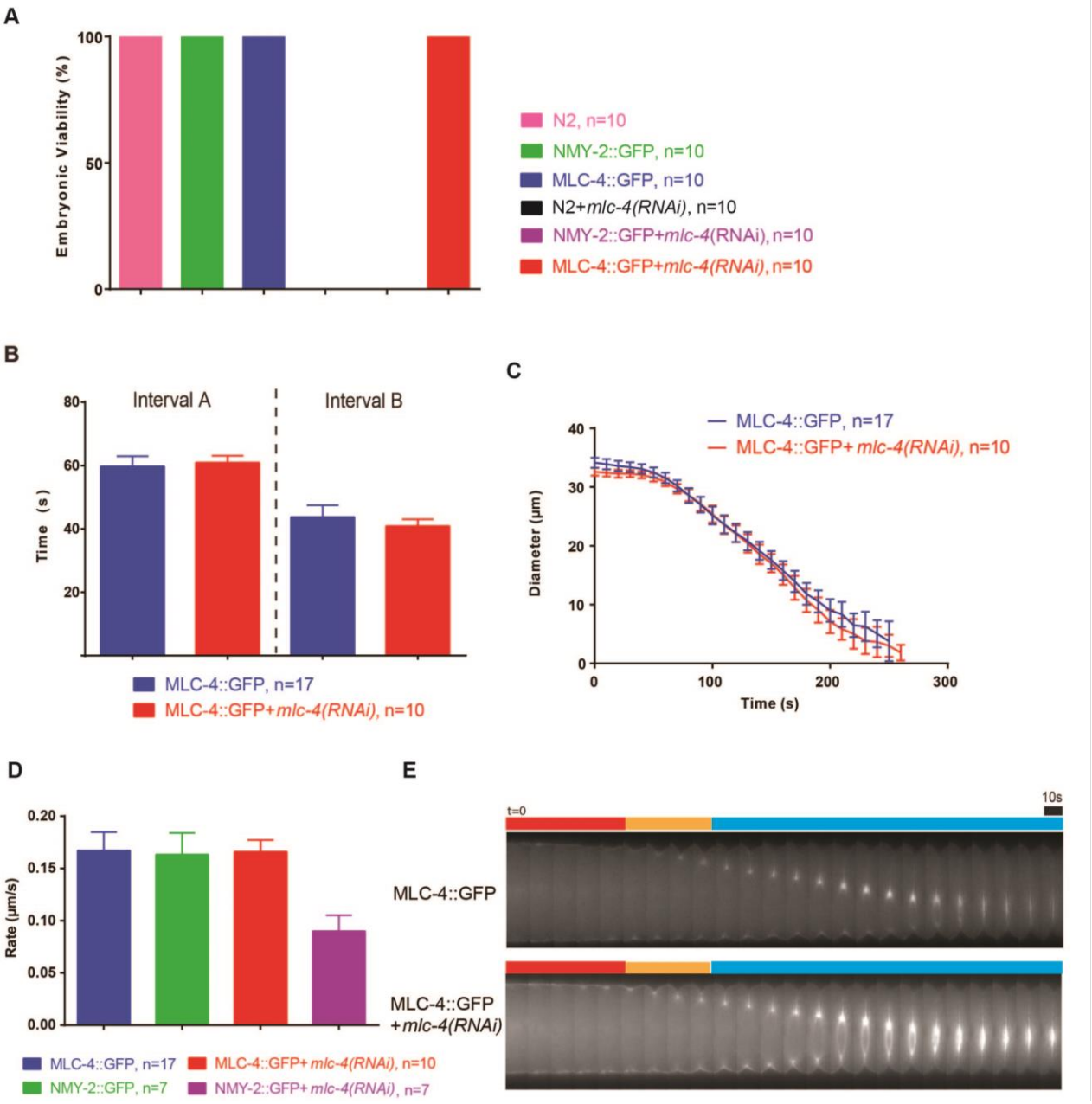

Figure 5 - MLC-4::GFP transgene is functional and is able to rescue the depletion of endogenous MLC-4. (A) Embryonic viability in worms expressing wild-type MLC-4::GFP in the presence (blue) or absence (red) of endogenous MLC-4 at 25-38 hours post-*mlc4(RNAi)* injection. Wild-type N2 worms (pink) and worms expressing NMY-2::GFP in the presence (green) or absence of endogenous MLC-4 (purple) were used as controls. (B) Contractile ring assembly was evaluated by measuring intervals A and B in embryos expressing MLC-4::GFP in the presence (blue) or absence of endogenous MLC-4 (red) at 46-48 hours post-injection. (C) Mean contractile ring diameter is plotted versus time for embryos expressing MLC-4::GFP in the presence (blue) or absence of MLC-4 (red) at 46-48 hours post-injection. The blue curve represents the average of n=17 and the red curve the average of n=10 embryos. Time zero corresponds to anaphase onset. (D) Mean of constriction rate is shown for the following groups: embryos expressing MLC-4::GFP in

the presence (blue) or absence (red) of endogenous MLC-4 at 46-48 hours post-injection, and embryos expressing NMY-2::GFP in the presence (green) or absence (purple) of endogenous MLC-4 at 23-25 hours post-injection. (E) Representative montages of the furrow region during contractile ring assembly (red bar - interval A and orange bar - interval B) and constriction (blue bar) in embryos expressing MLC-4::GFP in the presence or absence of mlc-4 at 46-48 hours post-injection. Scale bar, 10s. Error bars represent 95% confidence intervals.

4.3. Generation of strains expressing MLC-4(T17S18AA)::GFP and MLC-4(T17S18DE)::GFP

Phosphorylation of the regulatory light chain on the residues Threonine17 and Serine18 is believed to control the contractility of actomyosin in smooth muscle and vertebrate non-muscle cells (Vicente-Manzanares et al., 2009, introduction section 1.2). To determine how these modifications are important for cytokinesis, we generated worm strains expressing MLC-4 mutants that cannot be phosphorylated or are constitutively phosphorylated on the two mentioned residues, using MosSCI. The idea is to compare cytokinesis in embryos expressing wild-type MLC-4::GFP (section 4.2), MLC-4(T17S18AA)::GFP (the non-phosphorylatable mutant) or MLC-4(T17S18DE)::GFP (the phosphomimetic mutant). As mentioned in the introduction section 1.4, all transgenes should be expressed at identical levels, as they will all integrate in the same genomic locus and all have the endogenous promoter and 3' UTR sequences.

The strategy followed was identical to that described in methods, section 3.2. We started by cloning the targeting constructs, which were in all identical to that of wild-type MLC4::GFP, except that they carried mutations 17A18A (non-phosphorylatable mutant) or 17D18E (phosphomimetic mutant) in the codons 17 and 18 of the *mlc-4* coding sequence (Figure 6). We injected the targeting constructs in worm gonads and obtained one viable strain expressing each of the mutants.

Using appropriate primers for PCR amplification (methods section 3.2.2, table 3), the strain expressing MLC-4(T17S18AA)::GFP was determined to be homozygous and the strain expressing MLC-4(T17S18DE)::GFP heterozygous for the transgene, as it only carried one copy of the transgene. Despite several trials, we were not able to isolate a homozygous strain for the phosphomimetic mutant.

Figure 6- Sequence alignment of MLC-4 wild-type, MLC-4(T17S18AA)::GFP (the non-phosphorylatable mutant) and MLC-4(T17S18DE)::GFP (the phosphomimetic mutant) from aminoacids number 1 to 20. Threonine17 and Serine18 codons (red box) were mutated in order to generate the phospho-mutants. To generate MLC-4(T17S18AA)::GFP Threonine17 (tgg codon) was mutated to Alanine17 (cgg codon), Serine18 (tcc codon) was changed to Alanine18 (cgg codon). To generate MLC-4(T17S18AA)::GFP Threonine17 (tgg codon) was mutated to Aspartic Acid17 (gac codon), Serine18 (tcc codon) was changed to Glutamatic Acid18 (gag codon).

4.3.1 MLC-4(T17S18AA)::GFP does not rescue embryonic viability

Next we tested, whether the non-phosphorylatable mutant was able to rescue embryonic lethality or not. Embryonic viability test has already been described in section 4.1. As shown in Figure 7A, as opposed to worms expressing wild-type MLC-4::GFP, worms expressing MLC-4(T17S18AA)::GFP laid non-viable embryos when endogenous MLC-4 was depleted. Similar to what we observed when we depleted MLC-4 in the strain expressing NMY-2::GFP (section 4.1) 38 hours after injection of the dsRNA against endogenous mlc-4, the mutant worms were sterile. These results show that the non-phosphorylatable mutant MLC-4(T17S18AA) was not able to rescue embryonic viability and led to worm sterility.

4.3.2 MLC-4(T17S18AA)::GFP localizes as wild-type protein

The cellular localization of MLC-4(T17S18AA)::GFP was also evaluated. The localization pattern was identical to that described for the wild-type MLC-4::GFP: in the cytoplasm and at the mitotic spindle at the time of anaphase onset (C1), at the equatorial cortical region during shallow

deformation (C2), at the furrow (C3) and in the contractile ring (tip of the furrow, C4) (Figure 7B). Consistent with previous results shown in section 4.2, the fluorescent signal of MLC-4(T17S18AA)::GFP increased when endogenous MLC-4 was depleted (Figure 7B, compare panel C1-4 with D1-4).

4.3.3 MLC-4(T17S18AA)::GFP expression results in cytokinesis slow-down and cytokinesis failure

To characterize cytokinesis when the source of MLC-4 is primarily non-phosphorylatable instead of the wild-type version, we imaged 1-cell embryos expressing MLC-4(T17S18AA)::GFP in the presence of endogenous protein (movie 3-left) or after its depletion. Embryos expressing MLC-4(T17S18AA)::GFP failed cytokinesis 35 hours after injection of dsRNA against endogenous mlc-4 (movie 3-middle). We next tried earlier time points after dsRNA injection to assess the cytokinesis phenotype in a situation where some of the endogenous MLC-4 is still present. Embryos expressing MLC-4(T17S18AA)::GFP were able to complete cytokinesis at 33 hours post-injection but did so in a much slower fashion than controls (Figure 7C, F and movie 3-right). When compared to embryos expressing wild-type MLC-4::GFP in the absence of endogenous MLC-4 or expressing MLC-4(T17S18AA)::GFP in the presence of lower levels of endogenous MLC-4, intervals A and B were three times and approximately twice as long, respectively (Figure 7C-D); the time required for contractile ring constriction was much extended (apparent completion of cytokinesis was only achieved 550s after anaphase onset); and constriction rate was twice as slow (0.08 µm/s compared to 0.16 µm/s) (Figure 7E-F). Similar to when we depleted MLC-4 in the strain expressing NMY-2::GFP, expression of MLC-4(T17S18AA)::GFP seems to lead to problems during the final stages of cytokinesis.

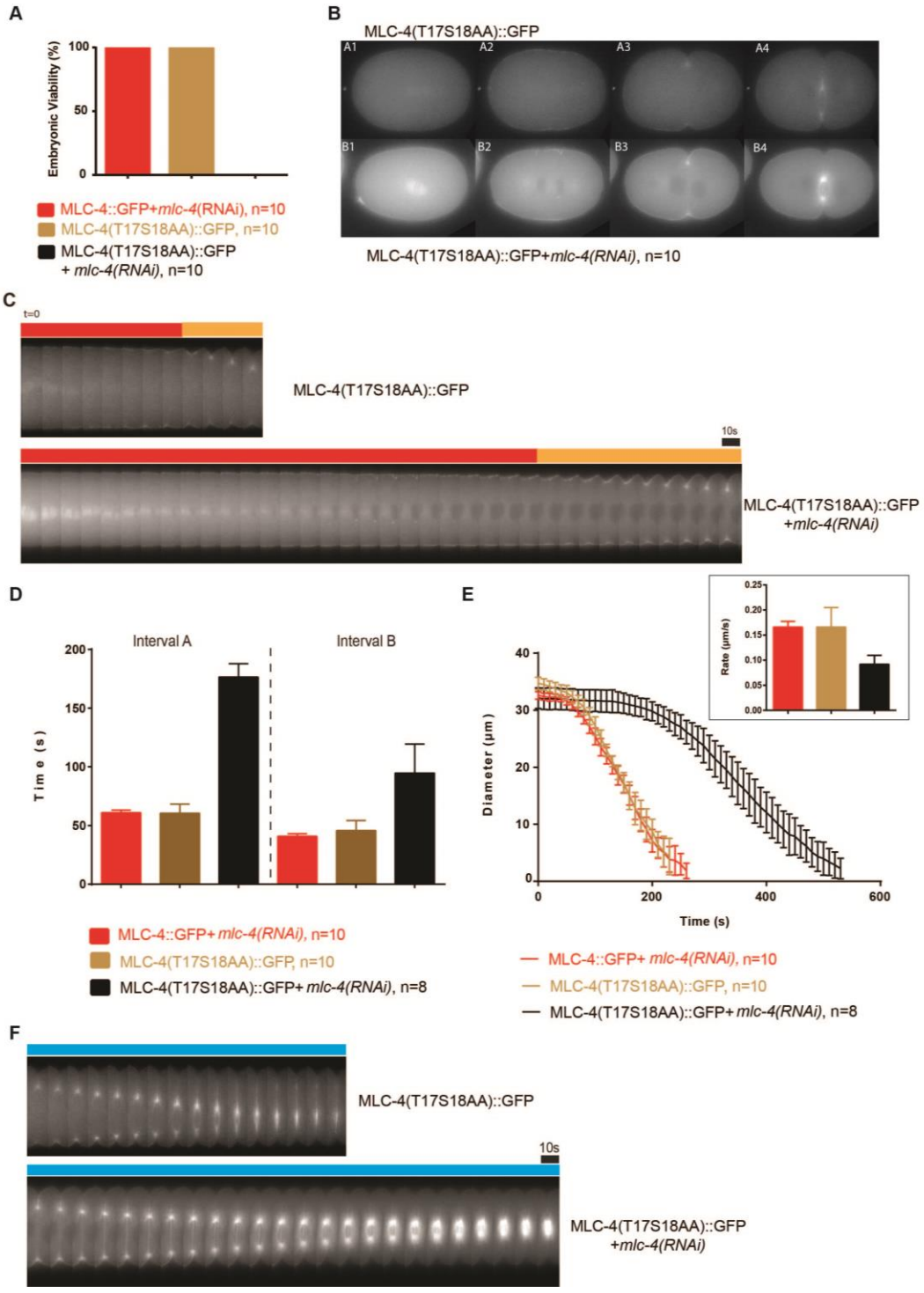

Figure 7 – MLC-4(T17S18AA)::GFP leads to non-viable embryos and cytokinesis slow-down. (A) Embryonic viability in worms expressing wild-type MLC-4::GFP in the absence of endogenous MLC-4 (red) and non-phosphorylatable MLC-4(T17S18AA)::GFP in the presence (brown) and absence of endogenous MLC-4 at 25-38 hours post-injection. (B) Worms expressing MLC-4(T17S18AA)::GFP were injected with dsRNA against endogenous mlc-4 and contractile ring assembly and constriction was followed in one-cell embryos at 33-35 hours post-injection. (C)

Representative montages of the furrow region during contractile ring assembly in embryos expressing MLC-4(T17S18AA)::GFP in the presence or absence of endogenous MLC-4,; red bar and orange bar represent intervals A and interval B, respectively. (D) Contractile ring assembly was evaluated by measuring intervals A and B in embryos expressing MLC-4::GFP in the absence of endogenous MLC-4 (red) and in worms expressing MLC-4(T17S18AA)::GFP in the presence (brown) or absence (black) of endogenous MLC-4. (E) Mean contractile ring diameter is plotted versus time for embryos expressing MLC-4::GFP in the absence of endogenous MLC-4 (red) and MLC-4(T17S18AA)::GFP in the presence (brown) or absence (black) of endogenous MLC-4. The red curve represents the average of n=10, the brown curve the average of n=10 and the black curve the average of n=8 embryos Time zero corresponds to anaphase onset. Mean of constriction rate is shown for the following groups: embryos expressing MLC-4::GFP in the absence (red) of endogenous MLC-4 at 46-48 hours post-injection, and embryos expressing MLC-4(T17S18AA)::GFP in the presence (brown) or absence (black) of endogenous MLC-4 at 33-35 hours post-injection (inset graph). (F) Representative montages of the furrow region during contractile ring constriction (blue bar) in embryos expressing MLC-4(T17S18AA)::GFP in the presence or absence of endogenous MLC-4. Scale bars, 10s. Error bars are 95% confidence interval of the mean.

4.3.4 Expression of MLC-4(T17S18DE)::GFP leads to worm sterility

As explained in section 4.3, we did not succeed in generating an homozygous strain for the MLC-4(T17S18DE)::GFP transgene. The progeny of heterozygous worms was therefore looked at in more detail. All the embryos laid by heterozygous mothers were viable, which means that homozygous embryos expressing MLC-4(T17S18DE)::GFP can hatch. Some of the progeny grew to become normal looking adult worms - these should be heterozygous for MLC-4(T17S18DE)::GFP. Some were incapable of moving - these should be wild-type worms that have not integrated the transgene and therefore have not integrated the *unc-119* gene that allows the worms to move (see introduction Figure 6 for details). Some grew but were sterile - these should be the homozygous for MLC-4(T17S18DE)::GFP. When we depleted endogenous MLC-4, the situation was different. Until 38 hours post-injection, very few embryos were laid and none were viable. After 38 hours post-injection, no more embryos were laid because the worms became sterile. Although a more complete genotypic analysis will be necessary, our results indicate that 1) embryos homozygous for MLC-4(T17S18DE)::GFP are viable in the presence of endogenous MLC-4 but adults become sterile. In the absence of endogenous protein these embryos are non-viable; 2) embryos heterozygous for MLC-4(T17S18DE)::GFP are viable in the presence but non-viable in the absence of endogenous MLC-4; 3) wild-type embryos expressing MLC-4(T17S18DE)::GFP due to the maternal loading are also viable in the presence but non-viable in the absence of endogenous MLC-4.

4.3.5 MLC-4(T17S18DE)::GFP localizes as wild-type protein

The localization of MLC-4(T17S18DE)::GFP was next evaluated (Figure 8B). GFP positive embryos could be 1) heterozygous for MLC-4(T17S18DE)::GFP; 2) homozygous for MLC-4(T17S18DE)::GFP, or 3) wild-type expressing MLC-4(T17S18DE)::GFP because of maternal loading. We do not have a straightforward way of distinguishing them. In all of them, MLC-4(T17S18DE)::GFP localized as wild-type MLC-4::GFP (sections 4.2, Figure 5B and section 4.3.2, Figure 7B). However, in contrast to what happened in embryos expressing wild type MLC-4::GFP or mutant MLC-4(T17S18AA)::GFP (Figure 5B, 7B), the fluorescent signal of MLC-4(T17S18DE)::GFP did not always increase after depletion of endogenous MLC-4 (compare Figure 7B with Figure 8B).

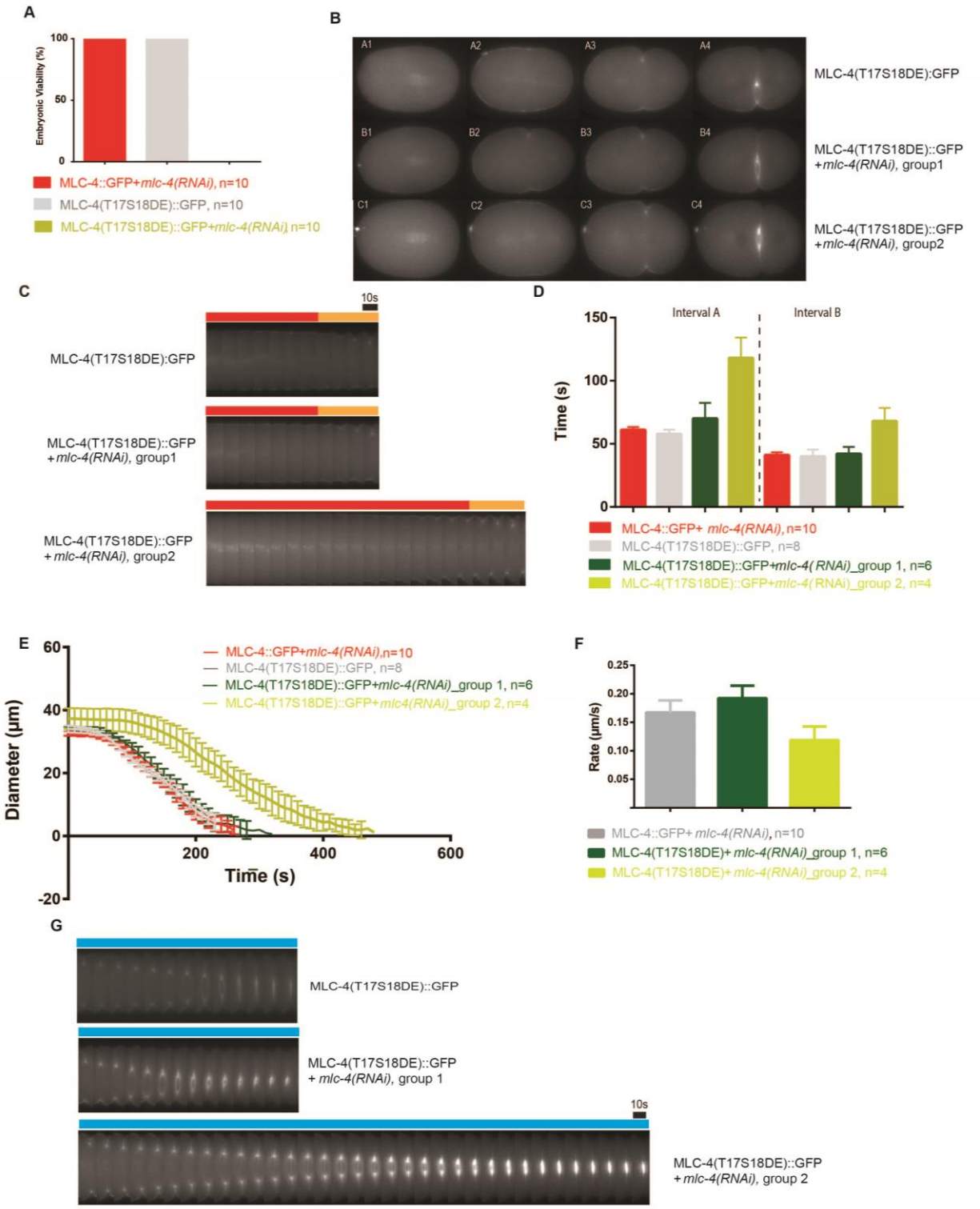

Figure 8 – Embryos heterozygous and homozygous for MLC-4(T17S18DE)::GFP, and wild-type embryos expressing MLC-4(T17S18DE)::GFP due to maternal loading are non-viable and may present prolonged but successful cytokinesis when endogenous MLC-4 is depleted. (A) Embryonic viability in worms expressing wild-type MLC-4::GFP in the absence of endogenous MLC-4 (red) and phosphomimetic MLC-4(T17S18DE)::GFP in the presence (grey) or absence of endogenous MLC-4. (B) Worms expressing MLC-

4(T17S18DE)::GFP were injected with dsRNA against mlc-4 and contractile ring assembly and constriction were followed in one-cell embryos at 27-33 hours post-injection. (C) Representative montages of the furrow region during contractile ring assembly in embryos expressing MLC-4(T17S18DE)::GFP in the presence or absence of endogenous MLC-4; red bar and orange bar represents interval A and interval B, respectively. (D) Contractile ring assembly was evaluated by measuring interval A and B in embryos expressing MLC-4::GFP in the absence of endogenous MLC-4 (red) and in worms expressing MLC-4(T17S18DE)::GFP in the presence (grey) or absence (dark green and yellow, group 1 and group 2 respectively) of endogenous MLC-4. (E) Contractile ring diameter plotted against time for embryos expressing MLC-4::GFP in the absence of endogenous MLC-4 (red) and MLC-4(T17S18DE)::GFP in the presence (grey) or absence (dark green and yellow, group 1 and group 2 respectively) of endogenous MLC-4. The red curve represents the average of n=10, the grey curve the average of n=10, the dark green curve the average of n=6 and the yellow the average of n=4 embryos. Time zero corresponds to anaphase onset. (F) Mean of constriction rate is shown for the following groups: embryos expressing MLC-4::GFP in the absence (red) of endogenous MLC-4 and embryos expressing MLC-4(T17S18DE)::GFP in the absence (dark green and yellow , group 1 and group 2, respectively) of endogenous MLC-4 (inset graph). (G) Representative montages of the furrow region during ring constriction (blue bar) in embryos expressing MLC-4(T17S18DE)::GFP in the presence or absence of endogenous MLC-4. Scale bars, 10 seconds. Error bars are 95% confidence interval of the mean.

4.3.6 Embryos expressing MLC-4(T17S18DE)::GFP successfully complete cytokinesis

In order to understand how expression of the phosphomimetic mutant MLC-4(T17S18DE)::GFP affects cytokinesis, 1-cell embryos for MLC-4(T17S18DE)::GFP were imaged undergoing first cell division. In the presence of endogenous MLC-4, all embryos expressing MLC-4(T17S18DE)::GFP complete cytokinesis with normal kinetics: interval A, interval B and rate of constriction are as those in embryos expressing wild-type MLC4::GFP (Figure 8C-F, movie 4-left). Interestingly, embryos depleted of endogenous MLC-4 completed cytokinesis successfully. The number of embryos laid in these conditions was very low and therefore it became difficult to increase the number of imaged embryos. Nevertheless, quantitative analysis of intervals A, B and constriction rate revealed two distinct results. Out of ten embryos, six show normal kinetics (group 1, movie 4-middle). The remaining four embryos showed a prolonged cytokinesis (group 2, movie 4-right). Interval A was twice as long as in controls. Interval B was also longer (70s compared to 40s). The time required for contractile ring constriction was much extended (cytokinesis was only achieved 450s after anaphase onset); and constriction rate was slow (0.12 µm/s compared to 0.16 µm/s). Curiously, these four embryos also showed prolonged final stages of constriction, indicating that they might have problems during abscission. The two types of behaviour obtained should reflect the different genotypes of embryos expressing the mutant MLC-4(T17S18DE)::GFP (homozygous or heterozygous embryos expressing for the MLC-4(T17S18DE)::GFP and wild-

type homozygous that expressed the phosphomimetic protein due to maternal loading. We have not been able to associate a specific phenotype to a genotype.

5. Discussion

The study of cytokinesis is a field with increasing importance, since evidence has accumulated over the last decades that cytokinesis failure can lead to several diseases, including cancer. Despite the increasing interest, cytokinesis still remains less understood than other stages of the cell cycle. In the present study, we examined how cytokinesis can be regulated by phosphorylation of the myosin regulatory light chain, an essential interacting partner of non-muscle myosin II - the motor that helps driving cytokinesis. Our experimental system was the *C. elegans* early embryo, which has been validated as a great system to quantitatively study cytokinesis *in vivo*.

5. 1 MLC-4 gradual depletion in one-cell C. elegans embryos results in cytokinesis slow-down, cytokinesis failure and worm sterility

NMII is a motor protein capable of generating force and translocating actin filaments. *In C. elegans*, NMII plays essential roles in multiple cellular and developmental processes starting from cytokinesis in the early embryo, to embryo elongation and later in the development of the gonad (Matsmura, 2005). NMII's critical contribution to cytokinesis has been proved by a variety of approaches, in a variety of systems (Matsmura, 2005).

The MRLC is one of the main regulators of the motor activity of NMII, as it binds to NMII's lever arm and when phosphorylated on the residues Threonine17 and Serine18 leads to the unfolding of the molecule, making it competent to establish interactions with other NMII molecules and consequently form bipolar filaments, which are essential for actomyosin contractility (Vicente-Manzanares, 2009).

MLC-4, a MRLC in *C. elegans* has been described as essential for cytokinesis (Shelton et al., 1999). We confirmed this result by depleting endogenous MLC-4 in 1-cell embryos expressing NMY2::GFP. Embryos fully depleted of MLC-4 did not assemble a contractile ring, and therefore multinucleated cells were generated. We were interested in understanding the contribution of MLC-4 to cytokinesis and for that we performed an RNAi time course experiment. Embryos partially depleted of MLC-4 were able to complete cytokinesis but took longer time than controls to do so. Intervals A and B were prolonged and constriction rate was lower than in controls, which indicates that MLC-4 contributes to both contractile ring assembly and constriction. In partial depletions, there is a reduced amount of endogenous protein MLC-4 available for the activation of NMII molecules, which supposedly results in a decreased number of bipolar filaments. Given

that NMII filaments are thought to contribute to generate the force that drives contractile ring constriction, a lower number of filaments should result in a slower cytokinesis. In agreement with this, we observed that NMY-2::GFP signal in the equatorial cortex during assembly of the ring and in the contractile ring during constriction was dimmer in MLC-4 partially depleted embryos than in control cells. The observation of NMY-2 aggregates in the cytoplasm might correspond to the extra NMII molecules that did not bind MLC-4. Indeed, biochemical studies have shown that an NMII mutant lacking the regulatory light chain binding site tends to aggregate *in vitro* (Trybus et al., 1991) and NMII aggregates have been observed in *D. melanogaster* oocytes and *S. pombe* upon MRLC deletion (Jordan and Karess, 1997).

MLC-4 partially depleted embryos were able to complete their first cell division but were unable to hatch, which means that something went wrong further along during embryonic development. Indeed, it has been shown that MLC-4 is required for embryonic elongation (Gally et al., 2009).

5.2 Wild-Type MLC-4::GFP probe is functional

In order to study the role of MLC-4 phosphorylation during cytokinesis, we generated a transgenic *C. elegans* strain expressing MLC-4 transgene tagged with a GFP probe using the MosSCI technique. The worms obtained expressed both endogenous MLC-4 from chromosome III and transgenic MLC-4 tagged with GFP from the chromosome II *Mos-1* locus. To analyse if the transgene was able to functionally replace the endogenous protein, we evaluated embryonic viability of the wild-type MLC-4::GFP strain upon depletion of endogenous MLC-4. Our results showed that MLC-4::GFP transgene is able to rescue embryonic viability. During cytokinesis MLC-4::GFP also performed as well as endogenous MLC-4. All the parameters analyzed for contractile ring assembly and constriction were similar in embryos expressing both endogenous and exogenous MLC-4 and embryos just expressing exogenous MLC-4. MLC-4::GFP localized very similarly to NMY-2::GFP in dividing 1-cell embryos: in the mitotic spindle, cortical equatorial region, furrow tip and mature contractile ring. This localization seems to be conserved among organisms as it has also been observed in *D. melanogaster* S2 cells, *H. pulcherrimus* eggs and HeLa cells (Shelton et al., 1999; Dean and Spudich, 2006; Uehara et al., 2008; Asano et al., 2009). In the absence of endogenous MLC-4, the MLC4::GFP signal intensity increased. This indicates that when the endogenous protein is present, its expression is preferred but upon its depletion the expression of MLC::GFP is forced.

Based on all our results, we can conclude that the MLC-4::GFP probe we generated is fully functional as it performs identically to endogenous MLC-4, as far as we can assess. The

careful characterization of the strain expressing wild-type MLC-4::GFP was very important because this was used as term of comparison for the strains expressing MLC-4 phospho-mutants.

5.3 Generation of strains expressing MLC-4(T17S18AA)::GFP and MLC-4(T17S18DE)::GFP

Multiple reports (Vicente-Manzanares et al., 2009) strongly suggest that the regulation of MRLC by phosphorylation on the residues Threonine17 and Serine18 is a key step for NMII regulation *in vitro*. However, its importance during cytokinesis *in vivo* is controversial. It seems to be crucial in *D. melanogaster* S2 cells, *H. pulcherrimus* eggs and HeLa cells but less important in *S. pombe* and unnecessary in *D. discoideum* (Ostrow et al., 1994; De la Roche et al., 2002; Lord and Pollard, 2004; Dean and Spudich, 2006; Uehara et al., 2008; Asano et al., 2009; Sladewski et al., 2009).

We decided to test the relevance of the above-mentioned phosphorylation during cytokinesis in our system where we can be sure that the phospho-mutants will be expressed at endogenous levels and we can accurately quantify several cytokinesis parameters. In fact, some of the prior studies conducted in other organisms involved over-expressed MLC-4 phospho-mutants, which complicates result interpretation (Uehara et al., 2008; Asano et al., 2009; Sladewski et al., 2009). Threonine17 and Serine 18 have been conserved evolutionarily and these residues are readily identified in all MRLCs we looked at.

Similar to what we did for MLC-4::GFP, we aimed to generate worm strains expressing a non-phosphorylatable version (MLC-4::T17S18AA), in which aminoacids 17 and 18 cannot be phosphorylated at any point of the cell cycle, and, a phosphomimetic version (MLC-4::T17S18DE) that mimics a continuous phosphorylation on 17 and 18 residues. We succeeded in generating a strain homozygous for MLC-4::T17S18AA and a strain heterozygous for MLC-4::T17S18DE. Both transgenes were engineered to be RNAi resistant, just like wild-type MLC-4::GFP.

5.4 MLC-4(T17S18AA)::GFP expression in one-cell C. elegans embryos leads to cytokinesis slow-down, cytokinesis failure, embryonic lethality and worm sterility

Given the assumed importance of the phosphorylation of MRLC on NMII activation and consequent bipolar filament formation and contractility, we expected embryos expressing MLC-

4(T17S18AA)::GFP to fail cytokinesis. We assessed cytokinesis phenotypes in 1-cell embryos expressing MLC-4(T17S18AA)::GFP in the presence or absence of endogenous MLC-4.

In the presence of endogenous MLC-4, embryos expressing MLC-4(T17S18AA)::GFP had no problems in progressing through cytokinesis and were all viable. MLC-4(T17S18AA)::GFP localized as wild-type MLC-4::GFP, indicating that T17S18 phosphorylation is not necessary for MLC-4 recruitment to the contractile ring. In the absence of endogenous MLC-4, embryos expressing MLC-4(T17S18AA)::GFP were not viable. This was expected because it has previously been shown that expression of such a mutant does not allow for embryonic elongation (Gally et al., 2009). 38 hours after injection of dsRNA against endogenous mlc-4, worms were sterile. 35 hours post-injection, all embryos failed cytokinesis. Cytokinesis failure also occurs when the equivalent non-phoshorylatable MRLC mutant is expressed in *D. melanogaster* S2 cells and *S. pombe*. In both cells, only a fraction of cells were incapable of completing cytokinesis (Dean and Spudich, 2006; Sladewski et al.,2009). Curiously, HeLa cells depleted of MRLC do not fail cytokinesis (Asano et al., 2009). The results of these studies are difficult to compare with ours for several reasons: 1) In S2 cells when the equivalent non-phoshorylatable MRLC mutant is expressed cytokinesis fails 25% of cases but also when the endogenous MRLC is depleted in wild-type cells. The level of endogenous MRLC expressed was around 5% (Dean and Spudich, 2006). In this study, the endogenous MRLC still present in low levels which can be enough to enable a fraction of successful cytokinesis. 2) In *S. pombe* and HeLa cells (Dean and Spudich, 2006; Sladewski et al.,2009), the transgenes are over expressed in presence of endogenous MRLC, which might not reflect the action of phospho-mutants. 33 hours post-injection, when more endogenous MRLC is available, embryos expressing MLC-4(T17S18AA)::GFP completed cytokinesis but this took longer than in controls. Cytokinesis slow-down has also been observed in previous studies in different experimental model systems (Dean and Spudich., 2006; Sladewski et al.,2009; Asano et al., 2009). However, the prolonged phase of contractile ring assembly was not observed in HeLa cells (Asano et al., 2009). This phenotypic evolution looks similar to that observed when endogenous MLC-4 was depleted in embryos expressing NMY-2::GFP. However, when we look at time scales, it became apparent that embryos that express MLC-4(T17S18AA)::GFP start failing cytokinesis at a later time point when less endogenous MLC-4 is present. 33 hours post-injection of mlc-4 dsRNA, all embryos not expressing MLC-4(T17S18AA)::GFP failed cytokinesis, while embryos expressing MLC-4(T17S18AA)::GFP did not. These results indicate that to some extent, expression of MLC-4(T17S18AA)::GFP is able to compensate for the reduction of endogenous MLC-4 levels, similar to what has been previously described in *S. pombe* (Le Goff et al., 2000; Naqvi et al., 2000). Unexpectedly, we showed that

expression of MLC-4(T17S18AA)::GFP results in prolonged last stages of constriction, which is indicative that MLC-4 phosphorylation in residues Threonine17 and Serine18 is important for the contractile ring-midbody ring transition. We also showed MLC-4 phosphorylation in Threonine17 and Serine18 is not crucial for proper localization as non-phoshorytalable MLC-4 localized as wild-type MLC-4 , In HeLa cells, non-phoshorytalable MRLC also localized normally (Asano et al., 2009) but in *D. melanogaster* S2 cells non-phoshorytalable MRLC did not localize in the equatorial cortex (Dean and Spudich, 2006).

Our results support the idea that Threonine17 and Serine18 MLC-4 phosphorylation is required for cytokinesis in *C. elegans*.

5.5 MLC-4(T17S18DE)::GFP expression in one-cell C. elegans embryos complete cytokinesis but are not viable

As mentioned before, we were able to isolate a worm strain expressing MLC-4(T17S18DE)::GFP from one chromosome II. Single homozygous worms expressing MLC-4(T17S18DE)::GFP could actually be isolated but they were sterile and did not allow for strain propagation. Embryos from heterozygous mothers have one (heterozygotes), two (homozygotes) or zero copies of MLC-4(T17S18DE)::GFP (but expressed MLC-4(T17S18DE)::GFP due to maternal loading). In the presence of endogenous MLC-4, all embryos were viable and in the absence of endogenous MLC-4 all were non-viable. In the absence of endogenous MLC-4, the number of embryos laid was in general very low and worms became sterile 38 hours post dsRNA injection. One-cell embryos expressing MLC-4(T17S18DE)::GFP, either heterozygously, homozygously or due to maternal loading, were analysed during cytokinesis. MLC-4(T17S18DE)::GFP localized as wild-type MLC-4::GFP. In the presence of endogenous MLC-4, embryos behaved as controls. In the absence of endogenous MLC-4, two distinct groups were observed. Embryos in group 1 behaved as controls. Embryos in group 2 completed cytokinesis but showed prolonged contractile ring assembly and prolonged last stages of constriction, when the ring is already small. Although we were not able to correlate embryo genotype with phenotype, the bimodal distribution of phenotypes suggests that the different levels of phosphomimetic protein expression could explain the different phenotypes. At the time we imaged the embryos after injection of dsRNA against endogenous mlc-4, all of them had the same amount of endogenous MLC-4 but different amounts of MLC-4(T17S18DE)::GFP. It is possible that group 1 corresponds to homozygous and group 2 to heterozygous embryos for MLC-4(T17S18DE)::GFP and wild-type homozygous embryos expressing the maternal loaded protein. Either half the

amount or the maternal load of MLC-4(T17S18DE)::GFP appears to be enough to allow for the completion of cytokinesis but not enough for it to occur with normal kinetics. Anyway, there may be other explanations therefore an increase of the number of embryos analyzed would be important. The fact that no embryos failed cytokinesis, strongly indicates that a constitutive state of phosphorylation of MLC-4 does not prevent cytokinesis from happening and that temporal regulation of NMII filament formation is not absolutely necessary during cytokinesis. This is in agreement with other studies in other organisms (Uyeda and Spudich, 1993; Dean and Spudich, 2006; Uehara et al., 2008; Asano et al., 2009). In light of our results, it is possible that NMII has to be in an active state (bound to phosphorylated MLC-4) during all cytokinesis.

In light of our results, it is possible that NMII has to be in an active state (bound to phosphorylated MLC-4) during all cytokinesis. Inactive state seems to not be relevant during the recruitment of contractile ring components to the cell equator and during abscission.

In slight contrast to other studies, MLC-4(T17S18DE)::GFP localized as wild-type MLC-4. In HeLa cells and in *D. melanogaster* S2 cells phosphomimetic MRLC showed preferential enrichment at the equatorial cortex when compared to the wild-type protein (Dean and Spudich, 2006; Asano et al., 2009). In *H. pulcherrimus* eggs, di-phosphorylated MRLC was not detected at the equatorial cortex before and shortly after the initiation of ingression (Uehara et al., 2008).

Embryos expressing MLC-4(T17S18DE)::GFP are able to complete cytokinesis but are not viable. This means that either later embryonic cytokinesis fail or other embryonic events that require acto-myosin contractility go awry. Embryonic elongation does require acto-myosin contractility but it has been shown that it happens normally in embryos expressing a phosphomimetic MLC-4 (Gally et al., 2009). Therefore, other embryonic events might be affected when phosphomimetic MLC-4 is expressed in *C. elegans*.

6. Conclusions and Future Perspectives

In conclusion, our data indicate that phosphorylation of MLC-4 on the residues Threonine17 and Serine18 is important for cytokinesis. When MLC-4 is not phosphorylated in these residues, cytokinesis does not happen. When MLC-4 is constitutively phosphorylated, cytokinesis completes similar to when wild-type MLC-4 is expressed. This suggests that once NMII bipolar filaments become competent for contractility by MLC-4 phosphorylation on residues Threonine17 and Serine18, they remain in the active state throughout cytokinesis. Our work also suggests an as-yet unexplored role for MLC-4 during the last stages of contractile ring constriction, which will have to be further studied.

Additionally, it will be important to investigate what goes wrong during embryonic development of MLC-4(T17S18DE)::GFP expressing embryos. Because, a problem in abscission might only be recognizable later, imaging of 1-cell embryos for longer periods of time should be conducted. In agreement with Shelton et al., 1999, we noticed that MLC-4 is highly expressed in the spermatheca and NMY-2 is not. In this specific context, MLC-4 must partner with NMY-1, the other non-muscle myosin II in *C. elegans* recently shown to be required for spermatheca functioning (Kovacevic et al., 2013). This together with the fact that depletion of MLC-4 leads to worm sterility, emphasizes the need to further characterize the roles of MLC-4 phospho-mutants in the spermatheca and gonad in order to understand the mechanics and relevance of acto-myosin contractility in these tissues.

7. References

Arnold, J.M. (1969). Cleavage furrow formation in a telolecithal egg (*Loligo pealii*). I. Filaments in early furrow formation. J. Cell Biol. *41*, 894–904.

Asano, S., Shi, Hamao, K., and Hosoya, H. (2009). Direct evidence for roles of phosphorylated regulatory light chain of myosin II in furrow ingression during cytokinesis in HeLa cells. Genes Cells *14*, 555–568.

Bosgraaf, L., and van Haastert, P.J.M. (2006). The regulation of myosin II in Dictyostelium. Eur. J. Cell Biol. *85*, 969–979.

Brenner, S. (1974). Caenorhabdztzs elegans. Genet. C. Elegans 71–94.

Burgess, S.A., Yu, S., Walker, M.L., Hawkins, R.J., Chalovich, J.M., and Knight, P.J. (2007). Structures of Smooth Muscle Myosin and Heavy Meromyosin in the Folded, Shutdown State. J. Mol. Biol. *372*, 1165–1178.

Byerly, L., Cassada, R.C., and Russell, R.L. (1976). The life cycle of the nematode Caenorhabditis elegans: I. Wild-type growth and reproduction. Dev. Biol. *51*, 23–33.

Carvalho, A., Desai, A., and Oegema, K. (2009). Structural Memory in the Contractile Ring Makes the Duration of Cytokinesis Independent of Cell Size. Cell *137*, 926–937.

Cassada, R.C., and Russell, R.L. (1975). The dauerlarva, a post-embryonic developmental variant of the nematode Caenorhabditis elegans. Dev. Biol. *46*, 326–342.

Conti, M.A., and Adelstein, R.S. (2008). Nonmuscle myosin II moves in new directions. J. Cell Sci. *121,* 11–18.

Craig, R., and Woodhead, J.L. (2006). Structure and function of myosin filaments. Curr. Opin. Struct. Biol. *16*, 204–212.

De Bono, M. (2003). Molecular approaches to aggregation behavior and social attachment. J Neurobiol, *54*, 78-92.

De La Roche, M., Smith, J., Betapudi, V., Egelhoff, T., and Côté, G. (2002). Signaling pathways regulating Dictyostelium myosin II. J. Muscle Res. Cell Motil. *23*, 703–718.

De Lozanne, A., and J. A. Spudich. (1987). Disruption of the Dictyostelium myosin heavy chain gene by homologous recombination. Science *236*, 1086– 1091.

Dean, S.O., and Spudich, J.A. (2006). Rho kinase's role in myosin recruitment to the equatorial cortex of mitotic Drosophila S2 cells is for myosin regulatory light chain phosphorylation. PLoS One *1*, e131.

DeBiasio, R.L., LaRocca, G.M., Post, P.L., and Taylor, D.L. (1996). Myosin II transport, organization, and phosphorylation: evidence for cortical flow/solation-contraction coupling during cytokinesis and cell locomotion. Mol. Biol. Cell *7*, 1259–1282.

Fire, A., Xu, S., Montgomery, M.K., Kostas, S. A., Driver, S.E., and Mello, C.C. (1998). Potent and specific genetic interference by double-stranded RNA in Caenorhabditis elegans. Nature *391*, 806–811.

Frøkjær-jensen, C., Davis, M.W., Hopkins, C.E., Newman, B., Thummel, J.M., Olesen, S., Grunnet, M., and Jorgensen, E.M. (2009). Single copy insertion of transgenes in C. elegans. Nat. Genet. *40*, 1375–1383.

Gally, C., Wissler, F., Zahreddine, H., Quintin, S., Landmann, F., and Labouesse, M. (2009). Myosin II regulation during C. elegans embryonic elongation: LET-502/ROCK, MRCK-1 and PAK-1, three kinases with different roles. Development *136*, 3109–3119.

Glotzer, M. (2005). The molecular requirements for cytokinesis. Science *307*, 1735–1739.

Green, R. A, Paluch, E., and Oegema, K. (2012). Cytokinesis in animal cells. Annu. Rev. Cell Dev. Biol. *28*, 29–58.

Guo, S., Kemphues, K.J. (1996). A non-muscle myosin required for embryonic polarity in Caenorhabditis elegans. Nature *382*, 455–58

Heckman, K.L., and Pease, L.R. (2007). Gene splicing and mutagenesis by PCR-driven overlap extension. Nat. Protoc. *2*, 924–932.

Heissler, S., and Manstein, D. (2013). Nonmuscle myosin-2: mix and match. Cell. Mol. Life Sci. *70*, 1–21.

Ikebe, M., and Hartshorne, D.J. (1985). Phosphorylation of smooth muscle myosin at two distinct sites by myosin light chain kinase. J. Biol. Chem. *260*, 10027–10031.

Ito, M., Nakano, T., Erdődi, F., and Hartshorne, D. (2004). Myosin phosphatase: Structure, regulation and function. Mol. Cell. Biochem. *259*, 197–209.

Jordan, P., and Karess, R. (1997). Myosin light chain-activating phosphorylation sites are required for oogenesis in Drosophila. J. Cell Biol. *139*, 1805–1819.

Jung, H.S., Komatsu, S., Ikebe, M., and Craig, R. (2008). Head–Head and Head–Tail Interaction: A General Mechanism for Switching Off Myosin II Activity in Cells. Mol. Biol. Cell *19,* 3234–3242.

Kamasaki, T., Osumi, M., and Mabuchi, I. (2007). Three-dimensional arrangement of F-actin in the contractile ring of fission yeast. J. Cell Biol*. 178*, 765–771

Kamm, K.E., and Stull, J.T. (2001). Dedicated Myosin Light Chain Kinases with Diverse Cellular Functions. J. Biol. Chem. *276,* 4527–4530.

Karess, R.E., Chang, X., Edwards, K.A., Kulkarni, S., Aguilera, I., and Kiehart, D.P. (1991). The regulatory light chain of nonmuscle myosin is encoded by spaghetti-squash, a gene required for cytokinesis in Drosophila. Cell *65*, 1177–1189.

Kimura, K., Ito, M., Amano, M., Chihara, K., Fukata, Y., Nakafuku, M., Yamamori, B., Feng, J., Nakano, T., Okawa, K., Iwamatsu, A., and Kaibuchi, K. (1996). Regulation of myosin phosphatase by Rho and Rho- associated kinase (Rho-kinase). Sci. *273*, 245–248.

Kovacevic, I., and Cram, E.J. (2010). FLN-1/Filamin is required for maintenance of actin and exit of fertilized oocytes from the spermatheca in C. elegans. Dev. Biol. *347*, 247–257.

Le Goff, X., Motegi, F., Salimova, E., Mabuchi, I., and Simanis, V. (2000). The S. pombe rlc1 gene encodes a putative myosin regulatory light chain that binds the type II myosins myo3p and myo2p. J. Cell Sci. *113*, 4157–4163.

Leal, A., Endele, S., Stengel, C., Huehne, K., Loetterle, J., Barrantes, R., Winterpacht, A., and Rautenstrauss, B. (2003). A novel myosin heavy chain gene in human chromosome 19q13.3. Gene *312*, 165–171.

Lee, C.-S., Choi, C.-K., Shin, E.-Y., Schwartz, M.A., and Kim, E.-G. (2010). Myosin II directly binds and inhibits Dbl family guanine nucleotide exchange factors: a possible link to Rho family GTPases. J. Cell Biol. *190*, 663–674.

Lord, M., and Pollard, T.D. (2004). UCS protein Rng3p activates actin filament gliding by fission yeast myosin-II. J. Cell Biol. *167*, 315–325.

Ma, X., Kovacs, M., Conti, M.A., Wang, A., Zhang, Y., et al. (2012). Nonmuscle myosin II exerts tension but does not translocate actin in vertebrate cytokinesis. Proc. Natl. Acad. Sci. USA *109*, 4509–14.

Mabuchi, I., and Okuno, M. (1977). The effect of myosin antibody on the division of starfish blastomeres. J. Cell Biol. *74*, 251–263.

Mabuchi, I., Tsukita, S., Tsukita, S., and Sawai, T. (1988). Cleavage furrow isolated from newt eggs: contraction, organization of the actin filaments, and proteincomponents of the furrow. Proc. Natl. Acad. Sci. U.S.A. *85*, 5966–5970.

Matsumura, F. (2005). Regulation of myosin II during cytokinesis in higher eukaryotes. Trends Cell Biol. *15*, 371–377.

Matsumura, F., Ono, S., Yamakita, Y., Totsukawa, G., and Yamashiro, S. (1998). Specific localization of serine 19 phosphorylated myosin II during cell locomotion and mitosis of cultured cells. J. Cell Biol. 140, 119–129.

Maupin P. and Pollard T. (1986). Arrangement of actin filaments and myosin- like filaments in the contractile ring and of actin-like filaments in the mitotic spindle of dividing HeLa cells. J. Ultrastruct. Mol. Struct. Res. *94*, 92–103.

Naqvi, N. I., Wong, K. C., Tang, X., and Balasubramanian, M. K. (2000). Type II myosin regulatory light chain relieves auto-inhibition of myosin-heavy- chain function. Nat. Cell Biol. *2*, 855–858.

Ostrow, B.D., Chen, P., and Biology, S. (1994). Expression of a Myosin Regulatory Light Chain Phosphorylation Site Mutant Complements the Cytokinesis and Developmental Defects of. J. Cell Biol. *127*, 1945–1955.

Piekny, A.J., and Mains, P.E. (2002). Rho-binding kinase (LET-502) and myosin phosphatase (MEL-11) regulate cytokinesis in the early Caenorhabditis elegans embryo. J. Cell Sci. *115*, 2271–2282.

Pollard, T.D., and Wu, J.-Q. (2010). Understanding cytokinesis: lessons from fission yeast. Nat Rev Mol Cell Biol *11*, 149–155.

Rankin, C.H. (2002). From gene to identified neuron to behaviour in Caenorhabditis elegans. Nat Rev Genet *3*, 622–630.

Sagona, A.P., and Stenmark, H. (2010). Cytokinesis and cancer. FEBS Lett. *584*, 2652–2661.

Sandquist, J.C., and Means, A.R. (2008). The C-terminal tail region of nonmuscle myosin II directs isoform-specific distribution in migrating cells. Mol. Biol. Cell *19*, 5156–5167.

Schroeder, T.E. (1968). Cytokinesis: filaments in the cleavage furrow. Exp. Cell Res. *53*, 272–276.

Schroeder, T.E. (1970). The contractile ring. I. Fine structure of dividing mammalian (HeLa) cells and the effects of cytochalasin B. Z. Zellforsch Mikrosk. Anat. *109*, 431–449

Schroeder, T.E. (1972). The contractile ring II. Determining its Brief Existence, Volumetric Changes, and Vital Role. J. Cell Biol *53,* 419-439.

Schroeder, T.E. (1975). Dynamics of the contractile ring. Soc. Gen. Physiol. Ser. *30*, 305–334.

Sellers, J.R., Pato, M.D., and Adelstein, R.S. (1981). Reversible phosphorylation of smooth muscle myosin, heavy meromyosin, and platelet myosin. J. Biol. Chem. *256* , 13137–13142.

Selman, G.G., and Perry, M.M. (1970). Ultrastructural changes in the surface layers of the newt's egg in relation to the mechanism of its cleavage. J. Cell Sci. *6*, 207–227.

Shelton, C.A., Carter, J.C., Ellis, G.C., and Bowerman, B. (1999). The Nonmuscle Myosin Regulatory Light Chain Gene mlc-4 is Required. J. Cell Biol. *146*, 439–451.

Sladewski, T.E., Previs, M.J., and Lord, M. (2009). Regulation of fission yeast myosin-II function and contractile ring dynamics by regulatory light-chain and heavy-chain phosphorylation. Mol. Biol. Cell *20*, 3941–3952.

Stiernagle, T. Maintenance of C. elegans (February 11, 2006), WormBook, ed. The C. elegans Research Community, WormBook, doi/10.1895/wormbook.1.101.1, http://www.wormbook.org

Trybus, K.M. (1989). Filamentous smooth muscle myosin is regulated by phosphorylation. J. Cell Biol. *109*, 2887–2894.

Tucker, J.B. (1971). Microtubules and a contractile ring of microfilaments associated with a cleavage furrow. J. Cell Sci. *8*, 557–571.

Uehara, R., Hosoya, H., and Mabuchi, I. (2008). In vivo phosphorylation of regulatory light chain of myosin II in sea urchin eggs and its role in controlling myosin localization and function during cytokinesis. Cell Motil. Cytoskeleton *65*, 100–115.

Uyeda, T.Q., Abramson, P.D., and Spudich, J.A. (1996). The neck region of the myosin motor domain acts as a lever arm to generate movement. Proc. Natl. Acad. Sci. U. S. A. *93*, 4459–4464.

Uyeda, T.Q., and Spudich, J.A. (1993). A functional recombinant myosin II lacking a regulatory light chain- binding site. Science. *262*, 1867–1870.

Vicente-Manzanares, M., Ma, X., Adelstein, R.S., and Horwitz, A.R. (2009). Non-muscle myosin II takes centre stage in cell adhesion and migration. Nat. Rev. Mol. Cell Biol. *10*, 778–790.

Wendt, T., Taylor, D., Trybus, K.M., and Taylor, K. (2001). Three-dimensional image reconstruction of dephosphorylated smooth muscle heavy meromyosin reveals asymmetry in the interaction between myosin heads and placement of subfragment 2. Proc. Natl. Acad. Sci. *98,* 4361–4366.

Wilkinson, S., Paterson, H.F., and Marshall, C.J. (2005). Cdc42-MRCK and Rho-ROCK signalling cooperate in myosin phosphorylation and cell invasion. Nat Cell Biol *7*, 255–261.

Woodhead, J.L., Zhao, F.-Q., Craig, R., Egelman, E.H., Alamo, L., and Padron, R. (2005). Atomic model of a myosin filament in the relaxed state. Nature *436*, 1195–1199.

Young, P.E., Richman, A.M., Ketchum, A.S., and Kiehart, D.P. (1993). Morphogenesis in Drosophila requires nonmuscle myosin heavy chain function. Genes Dev. *7*, 29–41.

Zang, J.H., Cavet, G., Sabry, J.H., Wagner, P., Moores, S.L., Spudich, J.A. (1997). On the role of myosin-II in cytokinesis: division of *Dictyostelium* cells under adhesive and nonadhesive conditions. Mol. Biol. Cell. *8*, 2617–29

Zarkower, D. Somatic sex determination (February 10, 2006), WormBook, ed. The C. elegans Research Community, WormBook, doi/10.1895/wormbook.1.84.1, http://www.wormbook.org

Zhang, P., McGlynn, A.C., West, C.M., Loomis, W.F., and Blanton, R.L. (2001). Spore coat formation and timely sporulation depend on cellulose in Dictyostelium. Differentiation *67*, 72–79.

Zhao, Z., and Manser, E. (2005). PAK and other Rho-associated kinases--effectors with surprisingly diverse mechanisms of regulation. . Biochem. J. *386*, 201–214.